2013-09-30

Rational Function and Distributed Two Block Architecture based Models for the Mitigation of Various Imperfections in Direct Conversion Transmitters

Aziz, Mohsin

UNIVERSITY OF CALGARY

Rational Function and Distributed Two Block Architecture based Models for the Mitigation of Various Imperfections in Direct Conversion Transmitters

by

Mohsin Aziz

A THESIS SUBMITTED TO THE FACULTY OF GRADUATE STUDIES IN PARTIAL FULFILMENT OF THE REQUIREMENTS
FOR THE DEGREE OF MASTER OF SCIENCE

DEPARTMENT OF ELECTRICAL AND COMPUTER ENGINEERING
CALGARY, ALBERTA

SEPTEMBER, 2013

Abstract

Nonlinearity in power amplifiers and in-phase and quadrature-phase (*I*/*Q*) imperfections in the transmitter are of enormous concern. Two models to alleviate these imperfections have been proposed. The first method employs a Rational Function based model for the joint mitigation of these impairments, while the second method is a Memory Polynomial based distributed two block model. The Rational Function model has an improvement of around 2 dB in NMSE and around 3 dB in ACEPR than the state of the art parallel Hammerstein based model. For the distributed two block model, we are able to reduce the complexity while maintaining reasonable performances. The number of coefficients and the number of floating point operations are reduced by around 17 percent, matrix conditioning is improved by 12-33 dB and the dispersion coefficient is reduced by 16-42 dB as compared to the previously proposed joint modulator and power amplifier nonlinearity compensation technique.

Acknowledgements

I would like to thank my supervisor Dr. Fadhel Ghannouchi for providing me with the opportunity to work under his guidance and trusting in me. I have learnt a lot under him and enjoyed every moment of my work in the iRadio laboratory. I would also like to thank my friends for their support.

I would also like to thank my parents and my brothers Dr. Hassan Aziz, Zain Aziz and sister Hijab. Thanks Javaria for your support.

Dedication

To my family

Contents

List of Tables

List of Figures

List of Symbols, Abbreviations and Nomenclature

Symbol	Definition
ACPR	Adjacent Channel Power Ratio
ACEPR	Adjacent Channel Error Power Ratio
ACI	Adjacent Channel Interference
AM-AM	Amplitude Modulation to Amplitude Modulation
AM-PM	Amplitude Modulation to Phase Modulation
DAB	Digital Audio Broadcasting
DVB-T	Digital Video Broadcasting – Terrestrial
DLA	Direct Learning Architecture
DPD	Digital Predistortion
DSP	Digital Signal Processing
FLOPs	Floating Point Operations
ILA	Indirect Learning Architecture
LMS	Least Mean Squares
LO	Local Oscillator
MFI	Mirror Frequency Imaging
MPM	Memory Polynomial
MSE	Mean Square Error
NMSE	Normalized Mean Square Error
PA	Power Amplifier
PD	Predistortion

PAE	Power Added Efficiency
PAPR	Peak to Average Power Ratio
PH	Parallel Hammerstein
WACP	Weighted Adjacent Channel Power
WCDMA	Wideband Code Division Multiple Access

Chapter one: Introduction

The importance of wireless communications in modern age is undeniable. The demand for highly efficient and reliable wireless communications systems poses new challenges in this field and a lot of research and development has been carried out to address these challenges. Wireless communications encompass a wide range of areas in electrical engineering. According to the library of parliament research publications, with the increase in the number of users moving to smartphones and other high data rate applications in Canada, there is dire need for research and developments in these areas [1], [2]. One key component in wireless communication systems is the power amplifier. As important as it is to develop highly efficient power amplifiers, equally important is the linearization of these. Behavioral modeling over the years has become an important tool for the linearization of the power amplifiers. A lot of literature concerning behavioral modeling of power amplifiers exists, some of the latest of which will be discussed throughout the thesis for the purpose of understanding the problems and the solutions to these problems and finally comparing them to the proposed models. In these works, various architectures for behavioral modeling can be found, concerning various issues related to the power amplifier characteristics such as nonlinearity, memory effects (short and long term) and many others.

This thesis places an emphasis on the behavioral modeling of power amplifiers in direct conversion transmitters to mitigate various imperfections introduced by the transmitter. Although detailed explanations of power amplifier modeling are present in literature, however in order to understand the basic idea of the work proposed one needs to start with the basis of power amplifiers modeling provided in the next section.

1.1 Need for modeling of power amplifiers

Power amplifiers exhibit nonlinear characteristics. A nonlinear system is one that does not satisfy the properties of superposition and scaling i.e. if

$$y_1(t) = T\{x_1(t)\} \tag{1.1}$$

and

$$y_2(t) = T\{x_2(t)\} \tag{1.2}$$

Then for any nonlinear system

$$\alpha y_1(t) + \beta y_2(t) \neq T\{\alpha x_1(t) + \beta x_2(t)\} \tag{1.3}$$

A power amplifier is an example of such a nonlinear system. Consider a power amplifier with input $x(t)$ and output $y(t)$. Then the relationship between the output and input to the power amplifier can be given by [3]

$$y(t) = f_{NL}(x(t)) \tag{1.4}$$

where f_{NL} is the nonlinear transformation function, or simply the response of the system to the input. Efficiency and linearity are the fundamental attributes relating to the design of a power amplifier. Highly efficient power amplifiers are being proposed to meet the demands of the consumers. But with high efficiency follows the degradation of linearity. Hence methods concerning improvement of linearity in power amplifiers hold a special place in systems where linearity is as important as efficiency. For this purpose modeling of power amplifier requires deep understanding. Generally classified into two groups namely, physical modeling and empirical modeling [3], [4], power amplifier modeling holds an enormous importance in modern wireless communication systems. The former requires knowledge of the PA active device and passive components to correctly model the power amplifier, while the later only requires the

nonlinear PA characteristics (i.e. input and output characteristics) to achieve the required model. In actual system it is not only the present value of time '*t*', that the output of the system depends upon, rather the past values of the input also affect the modeling function. This effect is called memory. A system with memory is given by [3]

$$f_{NL}\left(y(\mathrm{t}), \frac{dy(\mathrm{t})}{dt}, ..., x(\mathrm{t}), \frac{dx(\mathrm{t})}{dt}, ... \right) = 0 \tag{1.5}$$

A system having no effect of memory is termed a static system, while systems incorporating the effect of memory are called dynamic systems [3]. An important attribute in the design of power amplifiers is its efficiency, which is the measure of the ability of the power amplifier to convert the direct current power (P_{DC}) to RF power (P_{RF}). Drain efficiency is defined as [5]

$$\eta_{drain} = \frac{P_{RF,out}}{P_{DC}} \tag{1.6}$$

On the other hand, power added efficiency is defined as

$$\eta_{drain} = \frac{P_{RF,out} - P_{RF,\mathrm{in}}}{P_{DC}} \tag{1.7}$$

1.2 Imperfections in Direct Conversion transmitter

Direct conversion transmitters have gained enormous importance due to the desire for low cost and energy efficient transmitters. A detailed analysis on the architecture and performance of direct conversion transmitters is provided in [6], [7]. A block diagram of a direct conversion transmitter is shown in fig. 1.1. However, these transmitters suffer various problems at various stages in the architecture. Following are some of the major imperfections in direct conversion transmitters.

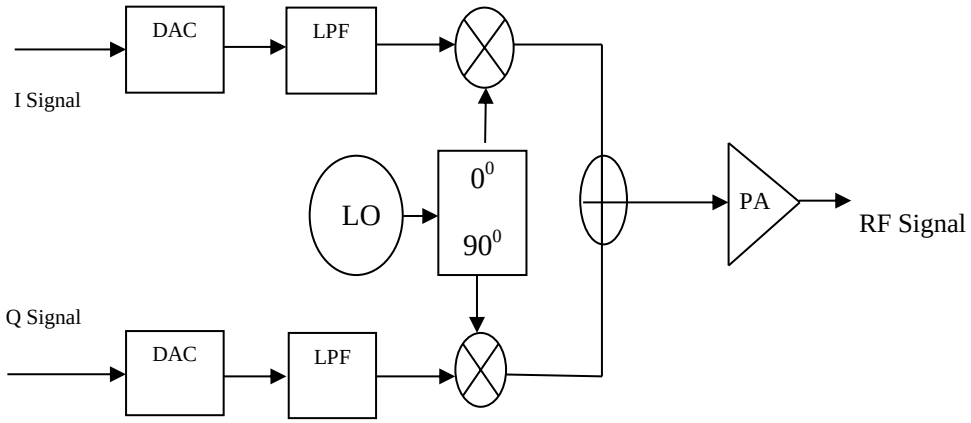

Figure 1.1: Typical architecture of a Direct Conversion transmitter

1.2.1 Power amplifier nonlinearity

Power amplifier is one of the most important and energy consuming part in an RF transmitter [5]. Linearity and efficiency are the main figures of merit related to the design of power amplifiers. Unfortunately, there is a trade-off between the two. As we increase the input power the efficiency increases linearly, however at a certain input power, the power amplifier reaches saturation and fails to exhibit linear characteristics. One of the main imperfections related to the power amplifiers is this nonlinear effect. The gain response of a class AB power amplifier is shown in fig. 1.2. It can be seen that for an increase in the input power, the gain remains constant to a certain value of the input, however as we increase the power further the gain drops, indicating the nonlinear behaviour of a power amplifier. Nonlinearity in power amplifiers leads to intermodulation distortions, which in turn give rise to spectral regrowth [8], [9]. This spectral regrowth can be seen in fig. 1.3. Generally, the third order inter modulations are more profound than the second order distortions, the mathematical basis for which is as follows [10].

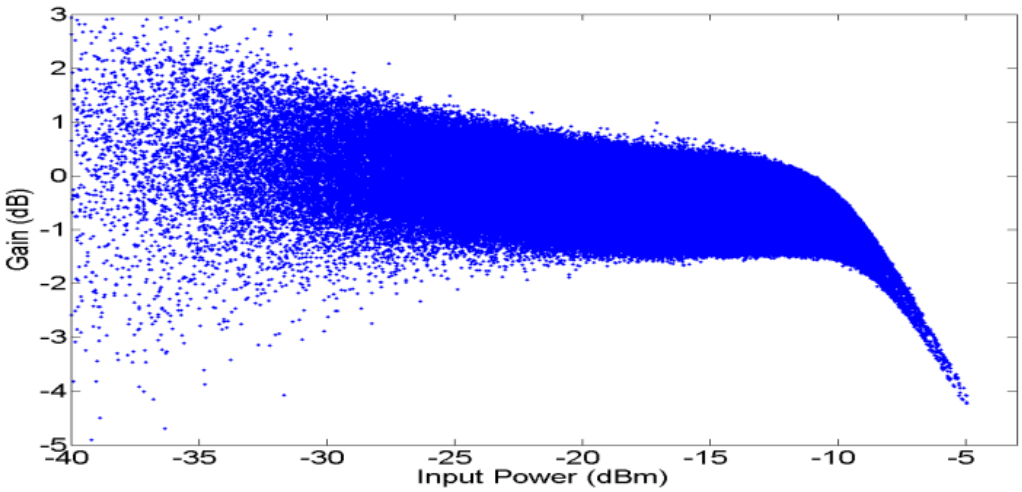

Figure 1.2: Gain characteristics of a class AB power amplifier for WCDMA 101 signal with a gain imbalance of 1.5 dB and phase imbalance of 3 degrees.

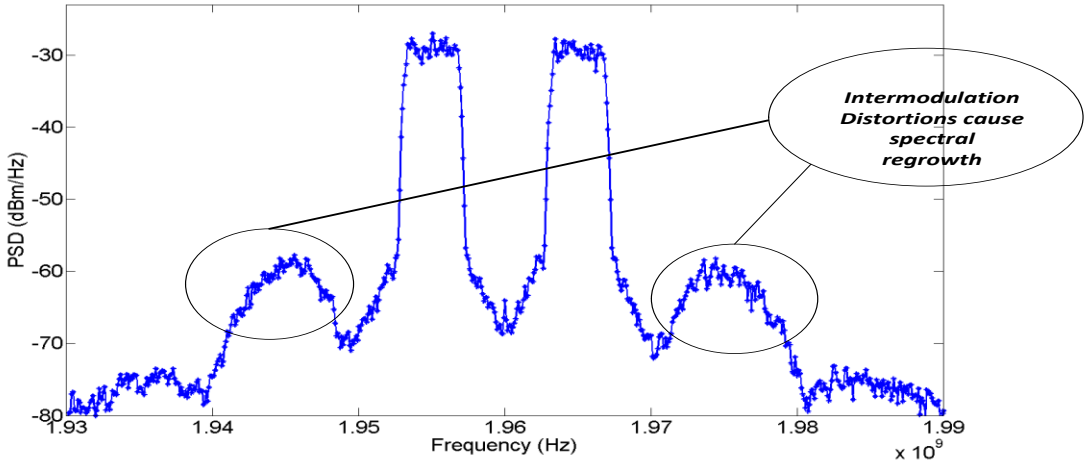

Figure 1.3: Intermodulation distortions or the nonlinear effect caused by the class AB power amplifier for WCDMA 101 signal.

Consider a power amplifier, which is fed by an input voltage $v_{in}(t)$, and produces an output voltage of $v_{out}(t)$. Since a power amplifier is a nonlinear device, the input-output relationship of such an amplifier can be given by

$$v_{out}(t) = \sum_i G_i v_{in}^i(t) \tag{1.8}$$

Considering only second and third order nonlinearities, the above equation can be written as [11]

$$v_{out}(t) = G_1 v_{in}(t) + G_2 v_{in}^2(t) + G_3 v_{in}^3(t) \tag{1.9}$$

If the input voltage has the form $A(t)cos(wt)$, where w represents the fundamental angular frequency of the input to the system, then the above equation becomes

$$v_{out}(t) = \underset{ideal\ \ response}{G_1 A(t)cos(wt)} + \underset{second\ \ order}{(1/2)\{G_2 A^2(t) G_2 A^2(t)cos(2wt)\}} + \underset{third\ \ order}{\{(1/4)G_3 A^3(t)cos(3wt) + (3/4)G_3 A^3(t)cos(wt)\}} \tag{1.10}$$

It can be seen from the above equation that the third order nonlinearity produces a component close by the fundamental frequency, which is unlike the second order nonlinearity. Hence the third order nonlinearity is more critical in PAs and hence this should be kept into consideration while designing and modeling power amplifiers. The dc part can be blocked by using a capacitor. Fig. 1.3 shows the intermodulation distortion caused by a class AB power amplifier for a WCDMA 101 signal. The encircled region shows the intermodulation distortion caused by the PA. In addition to this, the effect of memory in power amplifiers cannot be neglected. These memory effects degrade the performance of the transmitters if not accounted for, and manifest them as difference in the levels of the upper channel band and lower channel band. In terms of memory, PA modeling can be classified into following

1.2.1.1 Memoryless nonlinear models

In memoryless systems, the output depends only upon the present input samples and not on the previous input samples [14]. Such models exhibit frequency independent characteristics Consider an input $x(t)$ to a memoryless system and $y(t)$ be the output, which can be represented by

$$y(t) = f(x(t)) \tag{1.11}$$

The output y(t) of such a model depends only on one value of the input sample i.e. t. Various modeling techniques are present in literature to model such a behavior accurately. Some of these models are Saleh model (polar and quadrature), Modified Saleh models, Fourier series model, Bessel-Fourier models etc. [14]. Particularly, Saleh model [15] is one of the more commonly used models that can be used to model a memoryless nonlinear power amplifier. According to Saleh's polar model the AM/AM characteristics are given by

$$r_y(t) = f(r_x(t)) = \frac{a_1 r_x(t)}{1 + b_1[r_x(t)]^2} \tag{1.12}$$

The AM/PM is given by

$$\phi_y(t) = f(r_x(t)) = \frac{a_2 r_x(t)^2}{1 + b_2[r_x(t)]^2} \tag{1.13}$$

where a_1, b_1, a_2 and b_2 are the curve fitting parameters relating to the AM/AM and AM/PM characteristics.

1.2.1.2 Nonlinear models with memory

As mentioned earlier conventional memory-less nonlinear models are frequency independent models. However, in actual power amplifiers, the memory effects cannot be ignored as they show frequency dependent characteristics especially while using wideband signals where the bandwidth of the signal is comparable to that of the power amplifier [3].

1.2.2 In phase and quadrature phase imbalance

Another problem in the transmitter occurs due to the gain and phase mismatch introduced by the mixer between the in phase and quadrature components which occurs during the up-conversion

of the baseband signal to the carrier frequency. Consider an input signal to the transmitter of the form [16]

$$V_{in}(t) = A(t)\cos(w_c t + \phi(t)) \tag{1.14}$$

Here $A(t)$ and $\phi(t)$ represents time varying amplitude and phase respectively and w_c is the carrier frequency. In terms of in phase and quadrature components it can be written as

$$V_{in}(t) = I(t)\cos(w_c t) - Q(t)\sin(w_c t) \tag{1.15}$$

Where $I(t)$ and $Q(t)$ are the in phase and quadrature components respectively. In a typical transmitter such as the one shown in fig. 1.1, these I and Q signals pass through a digital-to analog converters with a sampling rate equal to the channel bandwidth. After converted into analog signals these are passed through a low pass filter to filter out the alias products. A local oscillator produces a 90 degree phase difference between the two branches which are then combined. However, all these components are not ideal, hence the output signal adopts the form given below

$$V_{out}(t) = (I(t) + d_i)\cos(w_c t) - \Delta\alpha(Q(t) + d_q)\sin(w_c t + \Delta\phi) \tag{1.16}$$

Where d_i and d_q are the in phase and quadrature dc offsets, and $\Delta\alpha$ and $\Delta\phi$ are the gain and phase imbalances, respectively. I/Q imbalance in transmitters causes Mirror Frequency Interference (MFI) resulting in adjacent channel interference [17, 18]. The mathematical expression for I/Q imbalances resulting in MFI is given in eqs. 1.17 and 1.20. For direct conversion transmitters, this image causes in-band distortion. Also these imbalances and local oscillator leakages tend to produce extra intermodulation distortions at the output, thus degrading the performance of the transmitter.

1.2.2.1 The *I*/*Q* imbalance model

As mentioned earlier, *I*/*Q* imbalance in direct conversion transmitters produces MFI. In order to fully understand this, one needs to derive the imbalance model. For this purpose, consider a base band signal *x*(t) provided as an input to a direct conversion transmitter. In terms of in phase and quadrature components, this signal can be written as $x_i(t)+jx_q(t)$. The effect of *I*/*Q* imbalance causes the signal to take the following form [18]

$$y(t) = g_1(t) * x(t) + g_2(t) * x^*(t) \tag{1.17}$$

Where

$$g_1(\mathrm{t}) = \frac{h_I(\mathrm{t}) + h_Q(\mathrm{t})\,\mathrm{g}e^{\mathrm{j}\phi}}{2} \tag{1.18}$$

$$g_2(\mathrm{t}) = \frac{h_I(\mathrm{t}) - h_Q(\mathrm{t})\,\mathrm{g}e^{\mathrm{j}\phi}}{2} \tag{1.19}$$

where g and ϕ represent the gain and phase imbalances introduced by the mixer, while $h_I(t)$ and $h_Q(t)$ represent the impulse responses due to the digital to analog converters and low pass filters. The conjugate term in the eq. (1.17) represents the formation of the image caused by the *I*/*Q* imbalance, In frequency domain, eq. (1.17) can be written as [18]

$$Y(w) = \mathrm{G}_1(w)\,\mathrm{X}(w) + \mathrm{G}_2(w)\,\mathrm{X}^*(-w) \tag{1.20}$$

The conjugate term causes the mirror frequency imaging (MFI).

1.3 Predistortion Techniques and related work

A block diagram of a typical digital predistortion setup is shown in fig. 1.4. In digital predistortion schemes, the basic idea is to create an inverse PA model. Consider the input to the PA as *x*(*t*) and the output as *y*(*t*), then the output can be expressed in terms of input as [19]

$$PA: y(\mathrm{t}) = \mathrm{c}_1 \mathrm{x}(\mathrm{t}) + \mathrm{c}_3\, x(\mathrm{t}) \,|\, x(\mathrm{t}) \,|^2 + \ldots\ldots\ldots \tag{1.21}$$

The inverse PA model (PA^{-1}) can be given by

$$PA^{-1}: x(\mathrm{t}) = d_1 y(\mathrm{t}) + d_3 y(\mathrm{t}) \,|\, y(\mathrm{t}) \,|^2 + \ldots\ldots\ldots \tag{1.22}$$

Several methods are found in literature, which address various imperfections in direct conversion transmitters. Various methods dealing with the PA nonlinearity such as parallel Hammerstein and Weiner models, two and three block models etc. have been mentioned in the previous sections while discussing various forms of nonlinear models. In terms of PA nonlinearity alone several methods have been proposed using various polynomials and architectures [20]-[25]. For *I*/*Q* imbalance compensation, [18] provides *I*/*Q* imbalance model given by eqs. 1.17 and 1.20 in the time and frequency domains. In addition to this, the authors have proposed two methods to mitigate this effect. The first method uses the second order statistics of the signals to estimate the predistorter parameters, while the second method uses widely linear (WL) least squares model fitting. The method proposed in [26] uses a Volterra series model to mitigate the effect of *I*/*Q* imbalance only. According to the authors, the method uses an inverse model for pre-compensation of the original baseband *I*/*Q* data. The model includes frequency dependent cross terms, which are nonlinear, between the *I* and *Q* branches. The authors have compared their model with other models present in literature such as [27], [28] and [29] and are able to achieve very high performance but at the expense of the number of coefficient. Hence it is a high complexity model. The method proposed in [30] uses pilot based compensation while the method in [31] applies online frequency domain adaptive predistortion to mitigate the effect of frequency dependent mismatches. All these methods [18, 26, 30, 31] consider the effect of *I*/*Q* imbalance

alone. However, there have been other methods which deal with these problems, i.e. power amplifier nonlinearity and *I*/*Q* imbalance. These methods form the back ground of the proposed work and are discussed in this section. A high performance state of the art model was presented in [32] where the authors have considered a Parallel Hammerstein model for the joint mitigation of *I*/*Q* imbalance and PA nonlinearity. The authors have used a memory polynomial based model for this purpose. This is an improvement over the previous proposed model [28], where the authors have considered a two block model where the first block compensates for the PA nonlinearity, while the second considers *I*/*Q* imbalance impairments. However, there is need for separate processing of these blocks, which in turn requires extra hardware [28, 32].

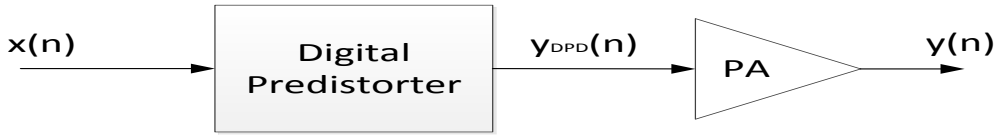

Figure 1.4: Digital Predistortion

1.4 Performance and complexity

The performance of a digital predistorter (DPD) is the measure of its ability to correctly model the inverse power amplifier characteristics. Some widely used figures of merit, which are also used in this thesis, to measure the performance of the DPD are the Normalized Mean Square Error (NMSE), Adjacent Channel Power Ratio (ACPR), Adjacent channel Error Power Ratio

(ACEPR). NMSE (dB) is a key measure of the in band performance of the predistorter is defined as [33, 34, 35]

$$NMSE = 10 \times \log_{10}\left(\frac{\sum_{k=0}^{N} |\mathrm{E}(k)|^2}{\sum_{k=0}^{N} |\mathrm{Y}_{\mathrm{measured}}(k)|^2}\right) \tag{1.23}$$

where $E(k)$ is the difference between the measured output and estimated output and N denotes the total number of samples. ACEPR on the other hand measures the out of band performance and is defined as [33, 34, 35]

$$ACEPR = \frac{\int_{Adj.Channel} |E(f)|^2 df}{\int_{Channel} |Y_{measured}(f)|^2 df} \tag{1.24}$$

Several methods are found in literature having very high performances in terms of NMSE and ACEPR. With the increasing demand in highly energy efficient systems, complexity and numerical stability of the predistorter is an important attribute of any model. In this thesis, complexity of the system is also given a major consideration along with the performance. Some of the main figures of merit in this regards are the number of complex valued coefficients, condition number and dispersion coefficient. Condition number is the measure of the sensitivity of the matrix inverse to slight disturbances or errors in the data. Condition number of a matrix **A** is defined as [36]

$$\kappa(\mathbf{A}) = \frac{\lambda_{\max}}{\lambda_{\min}} \tag{1.25}$$

Dispersion coefficient measures the number of bits required to completely fill the domain of the coefficient vectors and is defined as [33]

$$\chi(\mathbf{A}) = \frac{\max(|\mathbf{c}|)}{\min(|\mathbf{c}|)} \tag{1.26}$$

Where **c** is the vector of complex valued coefficients extracted from the model by using linear least squares method. Other important complexity metric is the number of floating point operations (FLOPs) required to compute various stages in the inverse modeling algorithm [37].

In the previous section, while discussing previous works several methods were proposed. Some considering only the intermodulation distortions created by the PA, others considered both the problems separately or jointly. In this regards, the complexity of the system becomes very important. Two block and three block architectures have been presented in literature to reduce the complexity of the system [33, 38]. In the two block model, the authors have proposed three twin nonlinear two box (TNTB) model architectures in which one of the blocks is static nonlinear block, while the other is a dynamic memory polynomial block. It is shown that by using the two block models the NMSE and the complexity of the system is reduced significantly as compared to the memory polynomial model. The method presented in [33] is a three block model where the first two blocks are static polynomials and the third block is a dynamic memory polynomial block. The authors have shown that by using the distributed model, the computational complexity of the system is reduced significantly. However, both these methods deal with the power amplifier nonlinearity and do not address the issue of *I*/*Q* imbalance. A high performance low complexity model presented in [32] is compared with the proposed methods as will be seen in the later chapters.

1.5 Thesis outline

Chapter one introduces and details various imperfections in direct conversion transmitters that have been dealt by in this work. It also introduces and explains various figures of merit required

to measure the performance and complexity of the proposed models. In chapter two, the first proposed model has been detailed. It introduces a Rational Function based model to mitigate various imperfections in direct conversion transmitters. Chapter 3 introduces a distributed model to deal with the aforementioned problems. Finally chapter four draws the conclusions and discusses various research problems and that can be dealt in the future. It also presents a literature review required for the future work.

Chapter Two: Rational function based model for the joint mitigation power amplifier mitigation and *I*/*Q* imbalance

2.1 Introduction

In chapter one of the thesis, it was mentioned that several polynomials can be used to model various digital predistortion models to compensate the effect of nonlinear dynamic power amplifier behavior. Some of these polynomial models are Volterra Series, Memory Polynomial, Envelope Memory polynomial, Generalized Memory Polynomial etc. A truncated Volterra series model is given by [26]

$$\begin{aligned} y(n) = & \sum_{m=0}^{M} a_m x(n-m) + \sum_{m_1=0}^{M} \sum_{m_2=m_1}^{M} a_{m_1 m_2} x(n-m_1)x(n-m_2) + \ldots\ldots\ldots\ldots \\ & + \sum_{m_1=0}^{M} \ldots\ldots\ldots\ldots\ldots \sum_{m_p=m_{p-1}}^{M} a_{m_1 m_2 \ldots\ldots m_p} x(n-m_1)\ldots\ldots\ldots\ldots x(n-m_p) \end{aligned} \tag{2.1}$$

where *M* indicates the memory depth and *a*'s are the coefficients or parameters of the model. A special and simplified case of the Volterra Series is the Memory Polynomial which is given by [33, 38]

$$y_1(n) = \sum_{m=0}^{M} \sum_{j=0}^{N} a_{m,j} x(n-m)\,|x(n-m)|^j, \quad x(.), y(.) \in \mathbb{C} \quad and \quad n, m, j \in \mathbb{N} \tag{2.2}$$

In this chapter we analyze the behavior of a Rational polynomial to mitigate the aforementioned imperfections in direct conversion transmitters. The use of rational function for predistortion can be found in literature [39, 42]. A paper presented in [39] compares various predistorter models based on their performances. It can be seen that the rational function based model gives the best performance in terms of NMSE as compared to the polynomial based PD, Radial Basis Function (RBF)-NN-Based PD and neuro-fuzzy based predistorter. However, their comparison is based

solely on the nonlinearity behavior of the power amplifier. In this chapter, we study the behavior of a Rational Function based model for the joint mitigation of *I*/*Q* imbalance and PA nonlinearity, keeping in mind both the performance and complexity of the system. *This work has led to the publication provided in [43]*.

2.2 Indirect Learning Architecture (ILA)

The techniques presented in this thesis are based on the indirect learning architecture [40], shown in fig. 2.1. A detailed analysis and comparison of direct and indirect learning architecture is presented in [2] and [40].

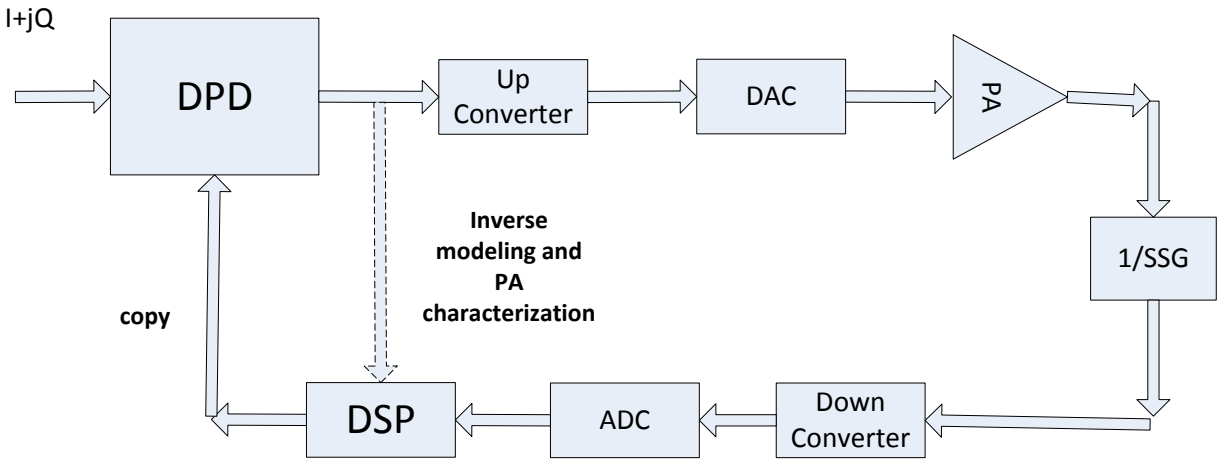

Figure 2.1: Block diagram of Indirect Learning architecture (@ 2012 M. Rawat [2])

2.3 Joint Mitigation of power Amplifier Nonlinearity and *I*/*Q* Imbalance using Parallel Hammerstein Model

One of the first models to compensate the effect of the PA nonlinearity and *I*/*Q* imbalance uses the parallel Hammerstein model and is presented in [32]. It is reasonably high performance model and the proposed models presented in this work are compared to it. Hence the author considers it important to explain this model in detail so as to understand how these impairments

have been mitigated by the aforementioned model. The basic implementation of the model presented in [32] is based on the conversion from the series structure presented in [28] to a parallel structure. The series model is shown in figs. 2.2 and 2.3. Fig. 2.2 shows various blocks in the architecture. It can be seen that first it compensates for the PA nonlinearity and then compensates for the *I*/*Q* imbalance, while fig. 2.3 shows the polynomial and filter transfer function required to achieve the predistortion model. However, this series structure has a drawback of separate processing of the two blocks i.e. separate processing for PA nonlinearity compensation and modulator impairments. It uses the following static nonlinear structure for PA nonlinearity compensation [32]

$$\psi_p(x_n) = \sum_{k \in I_p} a_{k,p} \mid x_n \mid^{k-1} x_n \tag{2.3}$$

Here p denotes the polynomial order from a set of $I_{p,}$ which can consider only odd orders or both, while x_n is the input to the model and k is the nonlinearity index. $| x_n |$ indicates the absolute value of the data $x_{n.}$, while $a_{\mathrm{k,p}}$ are the coefficients in the model required to create the inverse PA characteristics depending upon the nonlinearity index k and polynomial order p, and are given by [32]

$$a_{k,p} = (-1)^{(p-1)/2} \frac{\sqrt{\frac{(p+1)}{2}}}{[\frac{(k+1)}{2}]!} \left\{ \begin{matrix} \frac{(p-1)}{2} \\ \frac{(k-1)}{2} \end{matrix} \right\} \tag{2.4}$$

The above expression is for statistically orthogonal polynomials and the details are presented in [32].

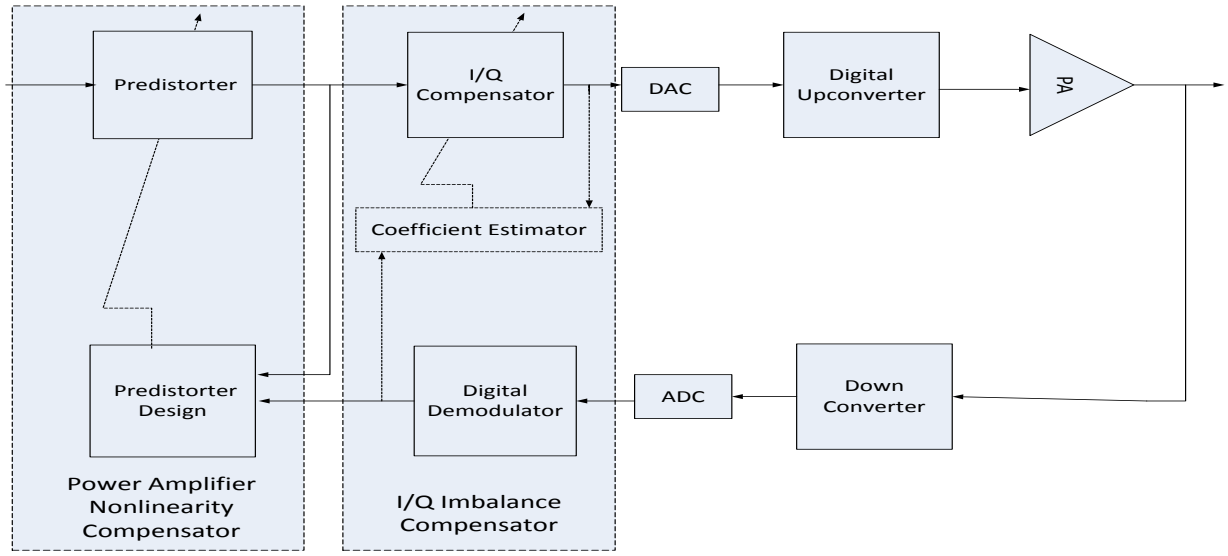

Figure 2.2: Power amplifier nonlinearity and *I*/*Q* imbalance compensation model presented in (@ 2008 IEEE [28])

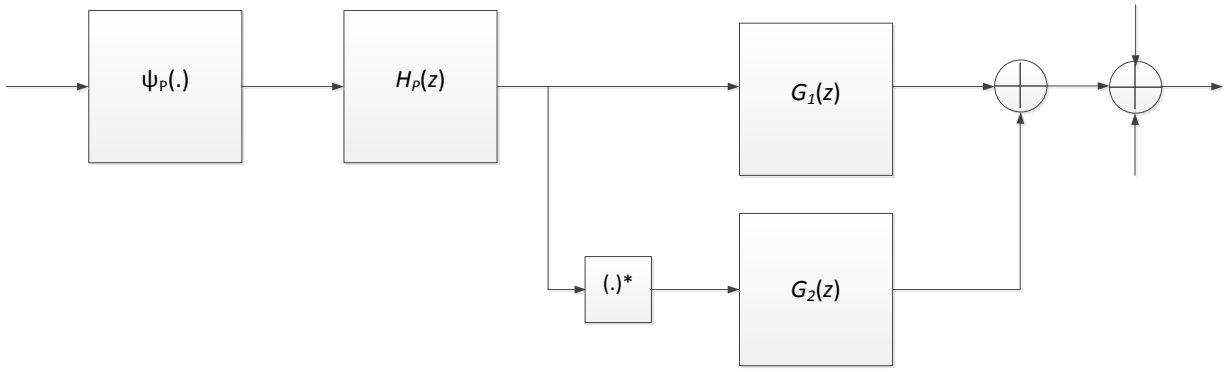

Figure 2.3: Block diagram of the two block model proposed in [28] (@ 2010 IEEE [32])

It can be seen in fig. 2.1, that the model compensates for the impairments (PA nonlinearity and *I*/*Q* imbalance) in the reverse order as they appear. After nonlinearity compensation, the actual signal is passed through a filter $G_1(z)$, while the conjugate of the signal is passed through $G_2(z)$. However, the authors in [32] have proposed a new architecture by changing this serial structure

into a parallel configuration as shown in figs. 2.4a and b. By combining the finite impulse response filter $H_p(z)$ and its conjugate $H^*_p(z)$ with the modulator imperfection compensator filters $G_1(z)$ and $G_2(z)$ respectively $F_p(z)$ and $F'_p(z)$ are generated which are given by

$$F_p(z) = H_p(z)G_1(z) \tag{2.5}$$

$$F'_p(z) = H^*_p(z)G_2(z) \tag{2.6}$$

At the final stage, as shown in fig. 2.4b, the conjugate is taken before the memory polynomial model i.e. the conjugate of the input signal is taken along with the actual input to form the following parallel combination of memory polynomial based predistorters

$$f(x_n) = \sum_{p=1}^{P} f_{p,n} * \psi_p(x_n) \tag{2.7}$$

$$f'(x_n^*) = \sum_{q=1}^{Q} f'_{q,n} * \psi_q(x_n^*) \tag{2.8}$$

Finally the two branches are combined to form the final model output given by

$$z_n = f(x_n) + f'(x^*_n) + c' \tag{2.9}$$

The final model architecture has been shown in fig 2.5. However, the authors in [32] have mentioned that by converting the series structure into parallel structure, the number of complex valued coefficients increase which increases the complexity of the system. The model has been simulated and measured for the purpose of comparison of the proposed models with this model. The results of the simulations have been detailed in tables 2.1 and 2.2.

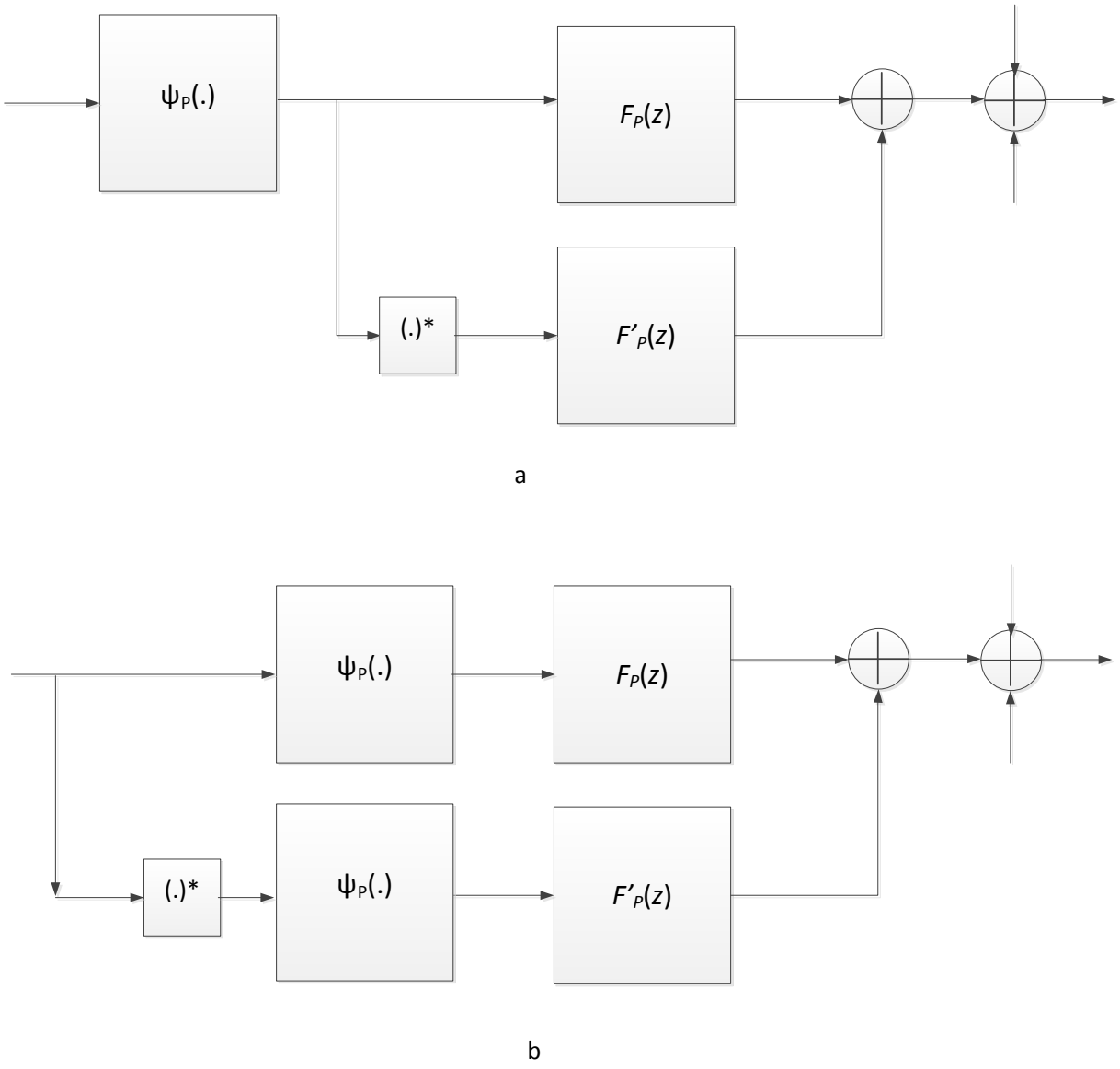

Figure 2.4: Conversion from serial architecture to a parallel configuration (@ 2010 IEEE [32])

2.4 Rational function based Model for Direct Conversion Transmitter Imperfections Compensation

Rational functions have been used for various purposes due to their ability as being good interpolators and extrapolators, along with them being universal approximators [39, 41, 42]. A

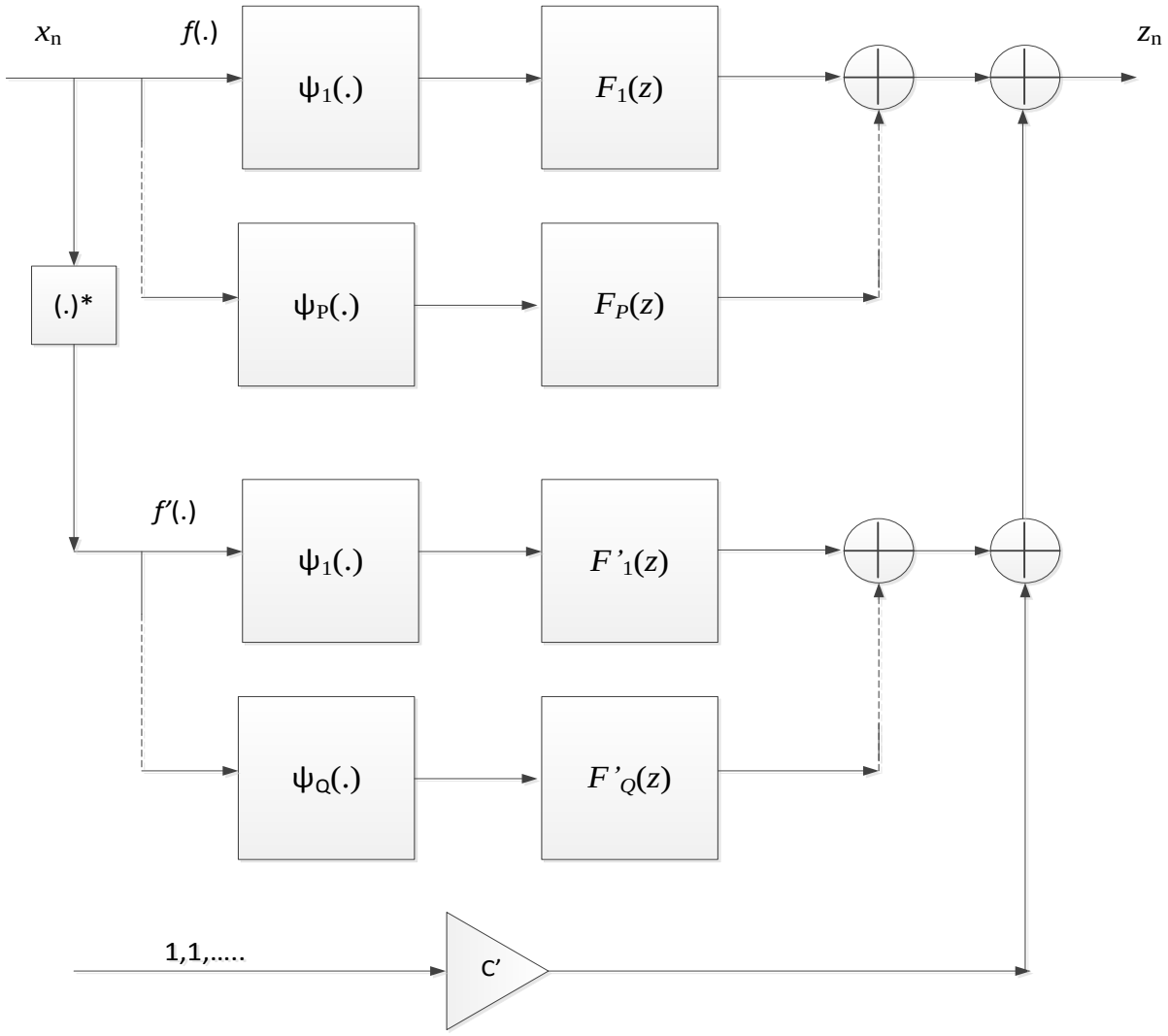

Figure 2.5: Final block diagram of the Parallel Hammerstein based model for the joint mitigation of PA nonlinearity compensation and *I*/*Q* imbalance (@ 2010 IEEE [32]).

static (memoryless) rational function is defined as the ratio of two polynomials which can be expressed as

$$y_{rational}(n) = \frac{\sum_{i=0}^{I} a_i x^i(n)}{\sum_{j=0}^{J} b_j x^j(n)}. \qquad (2.10)$$

i, j, a_i and b_j represent the order of the numerator and denominator and the coefficients of the model respectively, while $y_{rational}(n)$ and $x(n)$ are the output and input to the system respectively.

As mentioned earlier that the effect of memory in real systems cannot be ignored, hence if we consider the memory effect the above expression can be written as

$$y_{rational}^{'(n)} = \frac{\sum_{i=o}^{I}\sum_{m=o}^{M} a_{i,m} x(n-m)\,|\,x(n-m)\,|^{i}}{1+\sum_{j=1}^{J} b_j x(n)\,|\,x(n)\,|^{j}} \tag{2.11}$$

The above equation only considers the effect of dynamic nonlinear effects. Here m, $a_{i,m}$ and b_j denote the memory depth and the coefficients of the model respectively. If we compensate for the PA nonlinearity and I/Q imbalance the above function becomes

$$\mathbf{Y_{RF}} = \mathbf{H}\,\boldsymbol{\theta}_{\mathbf{RF}} \tag{2.12}$$

H is the matrix which takes into account the input signal $x(n)$ and output samples $y(n)$. For the mitigation of PA nonlinearity and I/Q imbalance, **H** matrix can be written as

$$\mathbf{H} = [\mathbf{h_1} \quad \vdots \quad \mathbf{h_1}^{*}] \tag{2.13}$$

To account for I/Q compensation, $\mathbf{h_1}^*$ has been appended to $\mathbf{h_1}$ matrix. Here h_1 is expressed as

$$\mathbf{h_1} = \begin{pmatrix} X_{i,0}(1) & \cdots & X_{i,M}(1) & -y(1)x(1)|x(1)| & \cdots & -y(1)x(1)|x(1)|^{J} \\ X_{i,0}(2) & \cdots & X_{i,M}(2) & -y(2)x(2)|x(2)| & \cdots & -y(2)x(2)|x(2)|^{J} \\ \vdots & & & & & \\ X_{i,0}(N) & \cdots & X_{i,M}(N) & -y(N)x(N)|x(N)| & \cdots & -y(N)x(N)|x(N)|^{J} \end{pmatrix} \tag{2.14}$$

Where the complex input vector is expressed as

$$X_{i,m}(N) = [x(N-m)\cdots\cdots x(N-m)\,|\,x(N-m)\,|^{i}] \tag{2.15}$$

$\boldsymbol{\theta_{RF}}$ is the vector of coefficients and can be extracted during training by the following expression

$$\boldsymbol{\theta}_{\mathbf{RF}} = \mathbf{H}^{-1}\mathbf{Y}_{\mathbf{RF}}. \tag{2.16}$$

From 2.16, it is clear that **H** matrix should be invertible. If this is not the case we can use pseudo inverse to find the inverse of matrix **H**. Singular value decomposition method is also used to calculate the inverse of the matrix. A least square approach to find $\boldsymbol{\theta}_{RF}$ is

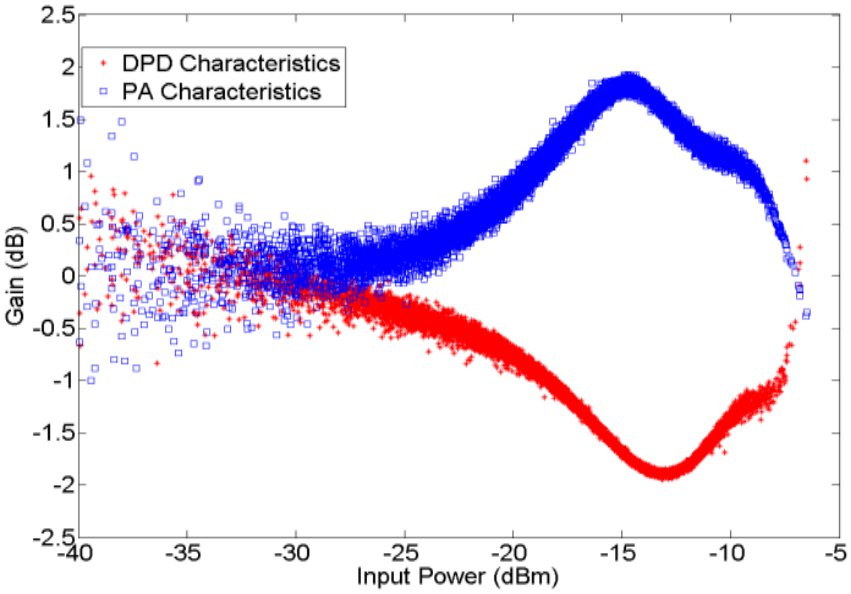

Figure 2.6: Gain characteristics of Rational Function based DPD model for a Doherty PA with no *I*/*Q* imbalance.

$$\hat{\boldsymbol{\theta}}_{RF} = (\mathbf{H}^{T}\mathbf{H})^{-1}\,\mathbf{H}^{T}\,\mathbf{Y}_{RF} \qquad (2.17)$$

2.5 Simulation results

The figures of merit for performance and complexity analysis are defined and detailed in chapter one of the thesis. The main figures of merit for performance evaluation are the NMSE, ACEPR and ACPR, while for complexity analysis condition number, dispersion coefficient and number of complex valued parameters. As mentioned earlier that it has been shown that rational function model for PA nonlinearity alone, attains the best NMSE as compare to other models. In this work, we wish to evaluate the performance of the rational function for the joint mitigation of PA nonlinearity and *I*/*Q* imbalance, problems that highly affect the performance and quality of direct conversion transmitters. The model was first tested for balanced data i.e. containing the effect of PA nonlinearity but not the in phase and quadrature phase imbalance. The balanced data was a Wideband Code Division Multiple Access (WCDMA) 11 signal for a Doherty power amplifier.

It can be seen in fig. 2.6 that the model is able to create an inverse PA model (as shown by the red curve). When the gain of the PA starts to drop, the model generates an increased gain to linearize the signal. However, in order to evaluate how accurately the model attains this behavior one needs to consider the NMSE (in band error evaluation criterion) and ACEPR (out of band error evaluation criterion). Table 2.1 shows that the proposed model attains an NMSE as low as -43.16 dB and an ACEPR as low as -56.75 dB. In order to show the improved and superior performance of the proposed model it is compared to the state of the art Parallel Hammerstein model [32]. It can be seen from table 2.1 that the proposed model has around 2 dB improvements in both the NMSE and ACEPR which is a reasonable improvement considering the fact that the Parallel Hammerstein model itself has a very high performance. Next, the model is tested for imbalanced data i.e. data containing the effect of *I*/*Q* imbalance along with the power amplifier nonlinearity. The imbalanced data is a WCDMA 101 signal for a class AB power amplifier having a gain imbalance of 1.5 dB and a gain imbalance of 3 degrees. Figs. 2.7 and 2.8 show the performance of the proposed model for such data. Fig. 2.7 shows the inverse modeling characteristics, for the proposed model and a model that does not account for *I*/*Q* imbalance, with respect to the input power. It can be seen that the proposed model (shown in green) correctly models the inverse PA characteristics as opposed to the other model (shown in red). Fig 2.8 shows the power spectral density of the non-linear and imbalanced PA output signal and the linearized signal generated by applying the proposed model. It can be seen that the proposed model is capable to linearize the signal significantly and attain an ACPR of greater than 50 dB. Figs 2.9 and 2.10 show the NMSE curves for the balanced and imbalanced data respectively, with respect to the nonlinearity orders of the numerator and denominator of the rational polynomial while keeping the memory depth 3. Figure 2.11 shows the error for the proposed and

PH model [32]. The effect of memory and nonlinearity (in the numerator and denominator) and the behaviour of rational functions has been elaborated in [51].

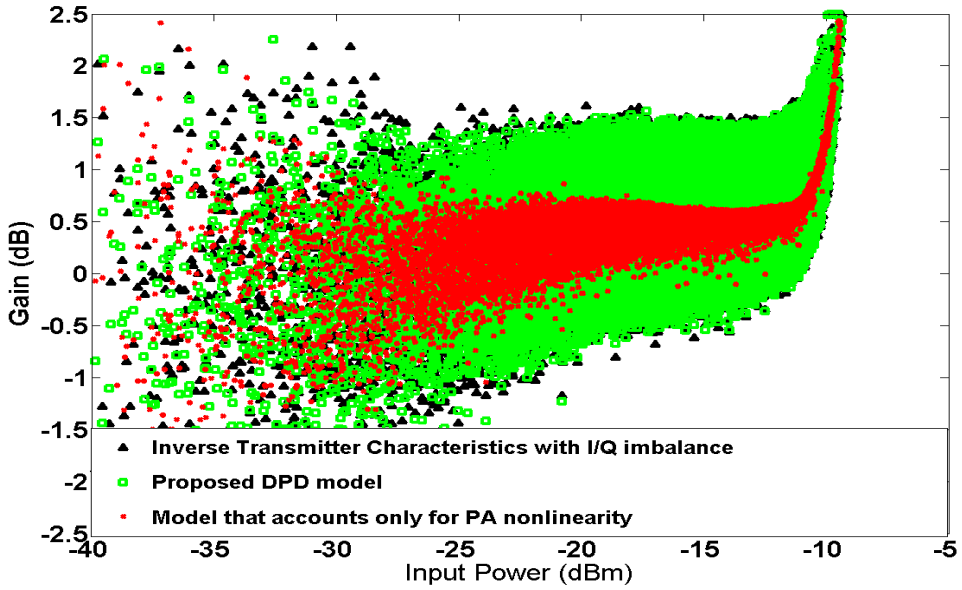

Figure 2.7: Gain characteristics of proposed model and its comparison to a model that does not account for *I*/*Q* imbalance (@ 2013 IEEE [43])

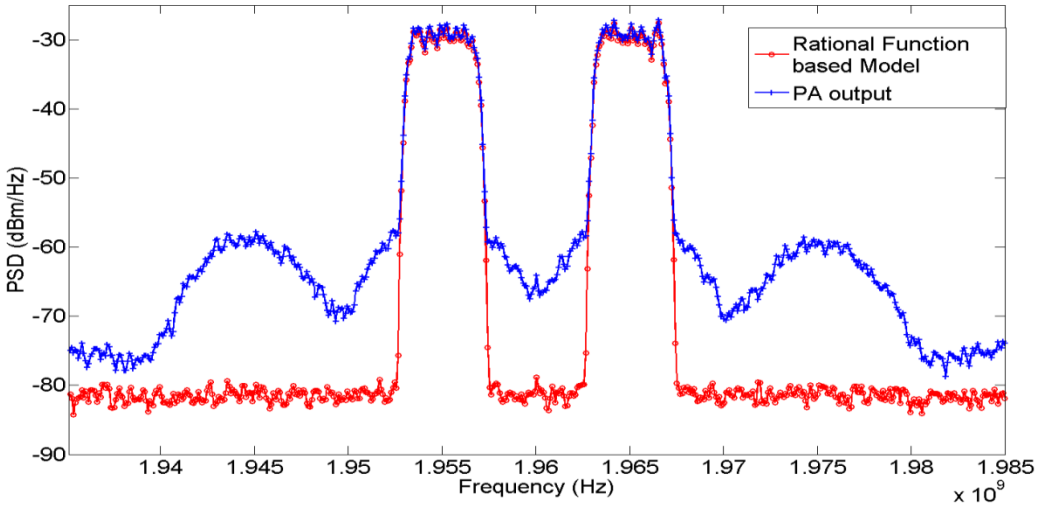

Figure 2.8: Power Spectral Density of the proposed model and the power amplifier output

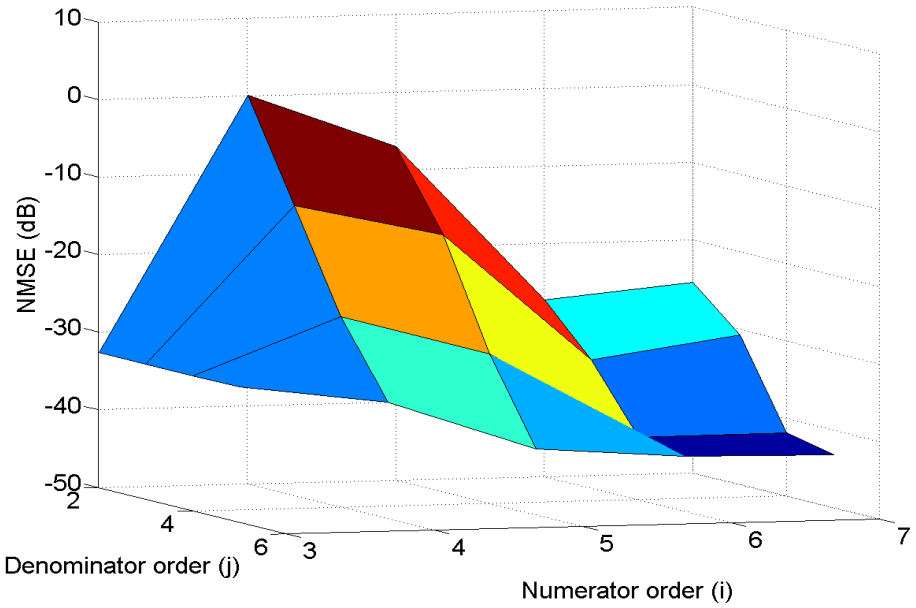

Figure 2.9: NMSE performance of the proposed model for WCDMA 11 balanced data for Doherty PA (@ 2013 IEEE [43])

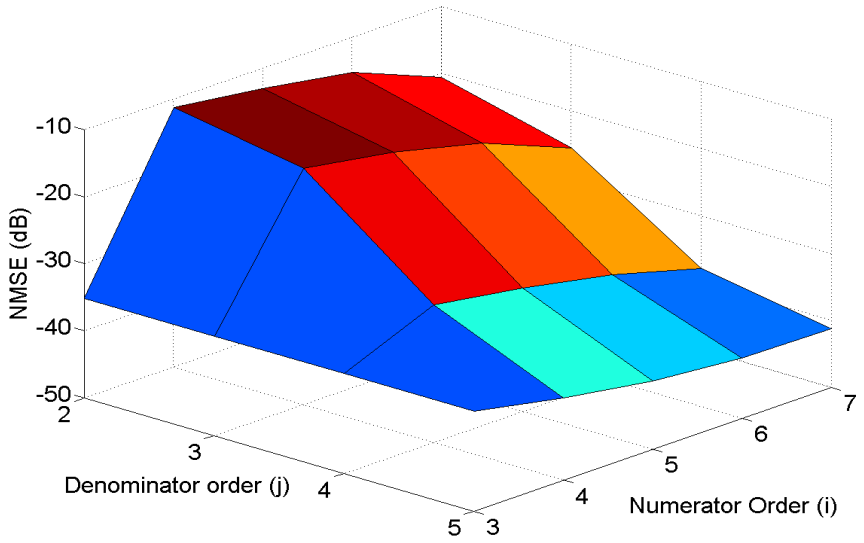

Figure 2.10: NMSE performance of the proposed model for WCDMA 101 imbalanced data for class AB PA (@ 2013 IEEE [43])

2.6 Complexity Analysis

As mentioned in the introduction, this thesis also places a great emphasis on the complexity of the digital predistortion models. The figures of merit to evaluate the complexity of the proposed Rational Function based model are the condition number, dispersion coefficient and the number of complex valued parameters required to compute the model. A larger value of all these quantities means a higher complexity or weaker numerical stability. These have been defined and detailed in chapter one of the thesis. Table 2.2 shows the complexity evaluation of the proposed model and its comparison to the Parallel Hammerstein model. Based on the results shown in Table 2.2 it can be seen that for the best modeling performance, the proposed model has higher complexity than the PH based model. However, the performance in terms of NMSE and ACEPR is better than the PH model. However, a trade-off is observed between performance and complexity. It can be seen that as the nonlinearity and memory depth of the proposed model are reduced, the performance of the model gets reduced *very* slightly, while the number of coefficients, dispersion coefficients and condition number is reduced significantly. For e.g., with

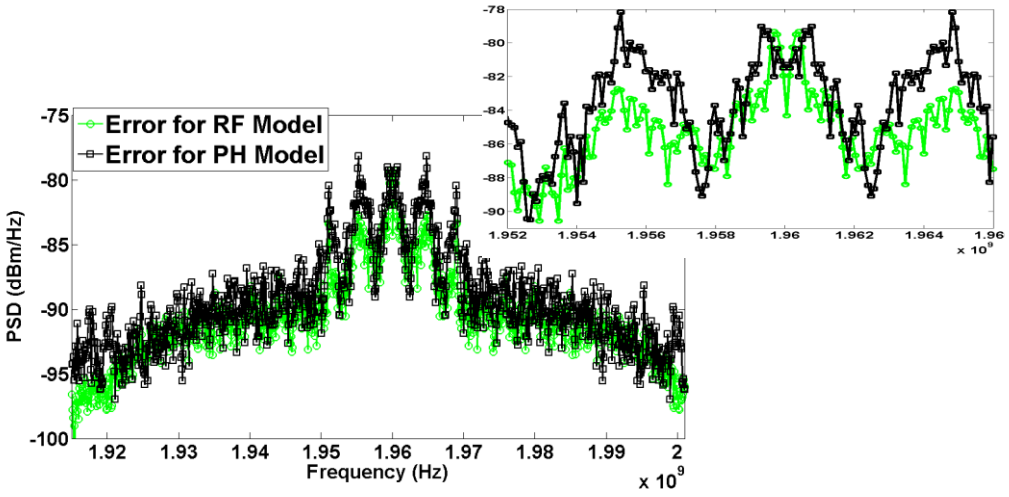

Figure 2.11: Error power spectrum density for proposed rational function model as well as PH model [32] using Wimax signal and class AB PA (@ 2013 IEEE [43])

the degradation of 1.37 dB in the NMSE, the number of coefficients reduced by 20 by reducing the memory depth and nonlinearity order.

2.7 Experimental setup and results

For measurement purpose, a class AB power amplifier is considered which is provided with a 20 MHz Wimax signal with Orthogonal Frequency Division Multiplexing (OFDM) based 64 Quadrature Amplitude Modulation (QAM) modulations. A gain imbalance of 1 dB and a phase imbalance of 3 degrees is created in the Wimax signal which is provided to the proposed model to produce the predistorted signal which is fed to a vector signal generator (Agilent E4438C). The linearized signal is captured using a vector signal analyzer (Agilent E4440A). It can be seen in Fig. 2.12, that the proposed model is able to linearize the system and attain a reasonable ACPR. The same procedure is repeated for the Parallel Hammerstein based model and it is observed that the proposed model had a 1 dB better ACPR than the state of the art Parallel Hammerstein based model. Hence the simulation and measurements show that the proposed rational function based model has a better performance than the state of the art parallel Hammerstein model with a slightly higher complexity.

2.8 Conclusion

In this chapter, a rational function based model for the joint mitigation of power amplifier nonlinearity and I/Q imbalance was proposed and explained. The model was evaluated for its performance and complexity. Simulation and measurement results validate that the model meets the design purpose. The model was compared to the parallel Hammerstein based model. It was shown that the model has a better performance in terms of NMSE, ACEPR and ACPR than the parallel Hammerstein model but with a slightly higher complexity.

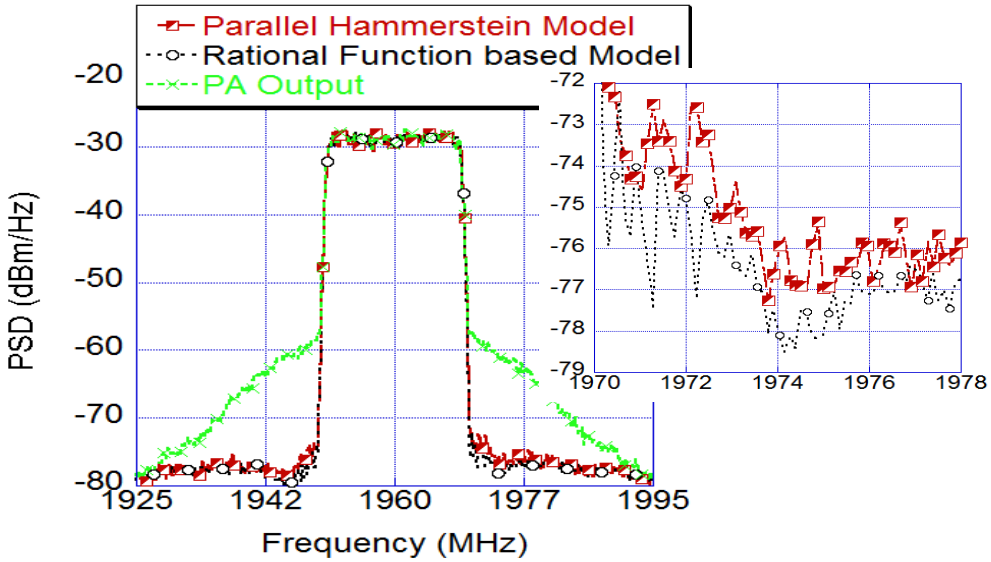

Figure 2.12: Measured performance of the proposed model and its comparison to the parallel Hammerstein model [32] (@ 2013 IEEE [43])

Table 2.1: Performance of the proposed model and its comparison to the Parallel Hammerstein based Model [32]. (@ 2013 IEEE [43])

Input Signal	Proposed Model		PH Model	
	NMSE (dB)	ACEPR (dB)	NMSE (dB)	ACEPR (dB)
WCDMA 11	-43.16	-56.75	-41.2	-54.29
WCDMA 101	-41.2	-53.42	-39.74	-50.19
WiMAX	-45.23	-55.08	-44.01	-52.7

Table 2.2: Complexity performance of the proposed model and its comparison to the Parallel Hammerstein based Model [32]. (@ 2013 IEEE [43])

Quadrature Independent Rational Function based model					
Order i/j/m	**NMSE (dB)**	**ACEPR (dB)**	**Dispersion Coefficient (dB)**	**Condition Number (dB)**	**No. of Coefficients**
7/5/3	**-41.2**	**-53.42**	**102.7**	**117.8**	**76**
6/4/3	**-41.01**	**-51.03**	**91.212**	**102.2**	**66**
5/3/3	**-39.815**	**-49.4**	**78.86**	**86.72**	**56**
5/4/2	**-39.83**	**-49.98**	**82.33**	**85.78**	**46**
5/3/2	**-39.82**	**-50.11**	**82.53**	**85.78**	**44**
Parallel Hammerstein based DPD Model					
NMSE (dB)	**ACEPR (dB)**	**Dispersion Coefficients (dB)**	**Condition Number (dB)**	**No. of Coefficients**	
-39.74	**-50.19**	**98.45**	**96.72**	**49**	

Chapter three: Low Complexity Distributed Model for the compensation of Direct Conversion Transmitter's Imperfections

3.1 Introduction

As mentioned in the previous chapters, the quality of a direct conversion transmitter is hugely affected by various imperfections at various stages in the transmitter. Some of these imperfections are the in-band and out-of-band distortions caused by the power amplifier, gain and phase imbalances in the modulator and leakages from the local oscillator. Chapter one describes the fundamentals of PA modeling and details various imperfections in the transmitter. Various models for the mitigation of various imperfections in transmitters have been provide in chapter one. Another model in [52] provides a single step identification along with a compound structure that considers these imperfections and it has been shown that the model work better than a GMP model. It also describes the importance of achieving low complexity along with better performance. Chapter two proposes a Rational Function based model which jointly mitigates the PA nonlinearity and *I*/*Q* imbalance, but is has been shown that although it has a reasonably performance than the state of the art model, its complexity is slightly higher. This chapter introduces and details a distributed memory polynomial based model with the aim of providing a low complexity model with reasonable performance. Distributed models have been presented in literature with the aim of reducing the complexity of the system [28, 33, 38, and 50]. Block diagrams of the method proposed in [28] has been provided in fig. 2.2, while figs. 3.1 and 3.2 provide the block diagrams for the methods proposed in [33] and [38]. The method proposed in [38] considers a two block model where one block is implemented by a memoryless nonlinearity LUT model, while the other is a lower order memory polynomial model. Using

these two blocks three different architectures have been proposed as shown in the figs. 3.1 (a), (b) and (c) and the authors have shown that the complexity in terms of the number of coefficients is reduced by 50 percent as compared to simple memory polynomial models. The authors in [33] have proposed a three blocks distributed model where the first two blocks are static polynomials while the third block is a dynamic memory polynomial.

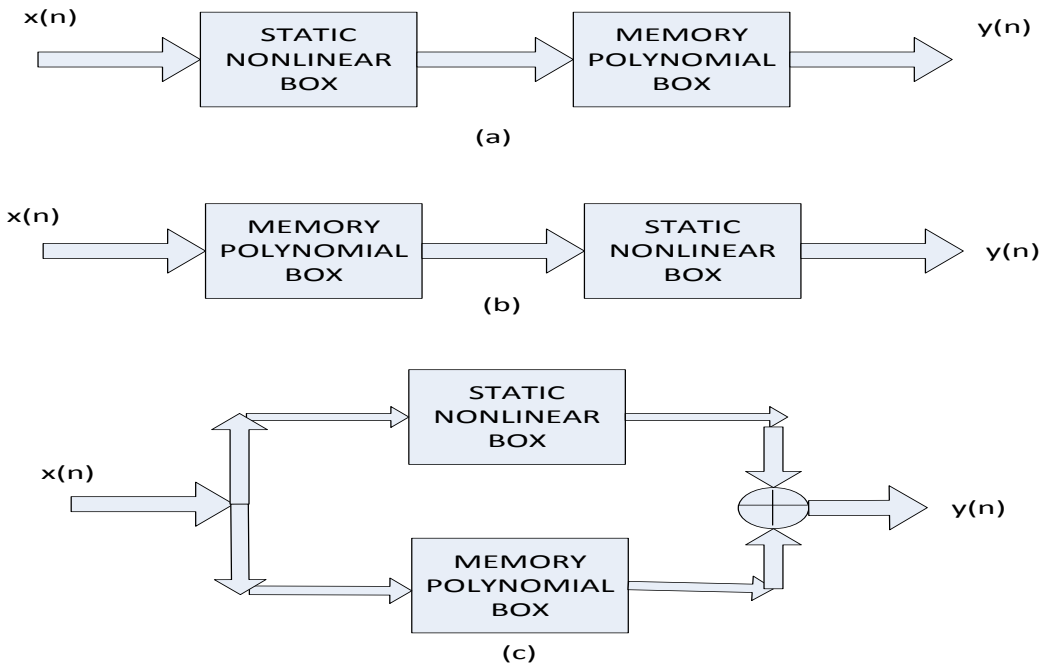

Figure 3.1: Block diagrams of the distributed two block models (a) forward twin nonlinear twin block model (b) reverse twin nonlinear twin block (c) parallel twin nonlinear twin block model presented in [38]

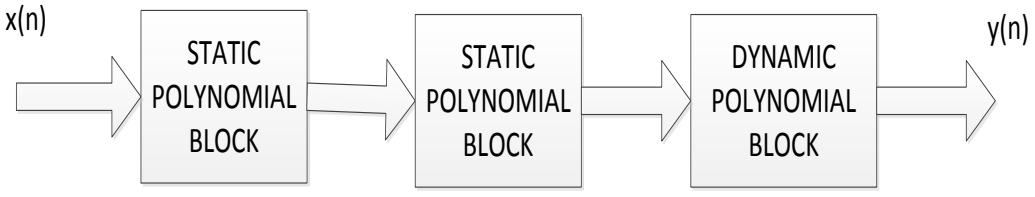

Figure 3.2: Block diagram of the three block model presented in [33]

The authors have shown that by employing this distributed structure, they have been able to reduce the condition number and dispersion coefficient as compared to a simple memory polynomial based model. Also the number of complex valued parameters has been reduced significantly. So these methods show that by distributed structures one is able to reduce the complexity of the system while maintain reasonable in-band and out-of-band performance. This forms the motivation behind this work. However, these methods only consider the effect of the PA nonlinearity and nothing is said about the effect of *I*/*Q* imbalance, which is a major problem in transmitters. In this regards models have been proposed which jointly or separately mitigate the effect of PA nonlinearity and *I*/*Q* imbalance. The method presented in [28] is a two block model where the first block alleviates the effect of PA nonlinearity and the second compensates the *I*/*Q* imbalance. The block diagram of this architecture has been shown in fig. 2.2. However, as reported in [32], the drawback of the method is that it requires extra hardware because of the separate processing of the two blocks. This is different form the proposed method where we adapt these blocks jointly using single step estimation requiring only one measurement for device characterization.

3.2 Distributed Two Block Model

The proposed distributed model for the compensation of imperfections in direct conversion transmitters consists of two blocks. The first block is a memory polynomial based block which aims to mitigate the effect of the dynamic power amplifier nonlinearity and hence has a high nonlinearity order. A memory polynomial is a pruned form of the Volterra series. For a Volterra series, the size of the complex valued coefficients increase exponentially with the nonlinearity order and memory depth. Hence various pruning strategies can be used to reduce the number of

coefficients. Memory polynomial is one such model which is less complex than a Volterra series model and is linear with respect to the model parameters [44] and hence is used in the first block. The second block, on the other hand, is a mildly nonlinear dynamic block to alleviate the effect of *I*/*Q* imbalance. A block diagram of the proposed model is provided in fig. 3.3. A memory polynomial with memory '*m*' and nonlinearity '*j*' is given by the following expression

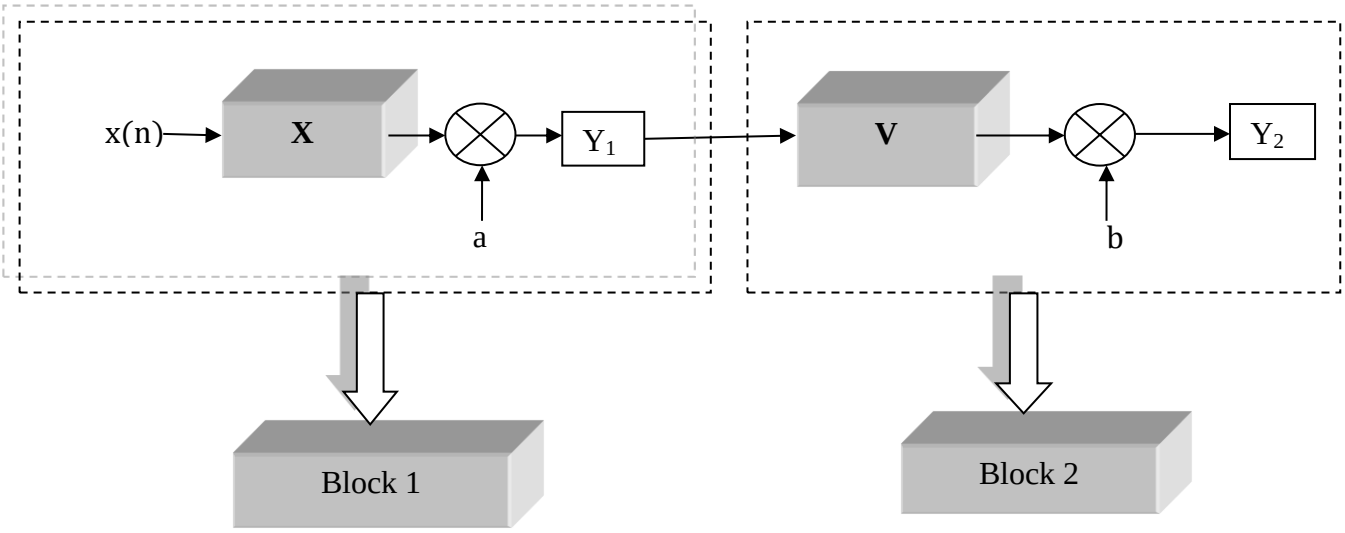

Figure 3.3: Block diagram of the proposed two block distributed model.

$$y_1(n) = \sum_{m=0}^{M} \sum_{j=0}^{N} a_{m,j}\, x(n-m)\,|x(n-m)|^{j}, \qquad x(.), y(.) \in \mathbb{C} \quad and \quad n, m, j \in \mathbb{N} \tag{3.1}$$

here $x(n)$ is the input to the memory polynomial model and $y_1(n)$ represents the output of the first block. N is the nonlinearity order and M is the memory depth while, $a_{m,j}$ are the complex valued coefficients of the model required to mitigate the effect of the PA nonlinearity. This memory polynomial creates an inverse PA model but does not account for the *I*/*Q* imbalance, for which the second block is designed. The output of the first block serves as the input to the second block which is a mildly nonlinear dynamic block to compensate for the effect of frequency dependent *I*/*Q* mismatch and residual nonlinearity and is given by the following expression

$$y_2(n) = \sum_{m'=0}^{M'} \sum_{k=0}^{K} (b'_k \, y_1(n-m') \,|\, y_1(n-m')|^k + c'_k \, y_1^*(n-m') \,|\, y_1(n-m')|^k) + LO \tag{3.2}$$

M' and K_1 represent the memory depth and the nonlinearity of the second block respectively while b'_k and c'_k are the complex values coefficients generated by the model to mitigate the effect of *I*/*Q* imbalance. LO term represents the LO leakage. In matrix notation, eq. 3.1 can be written as

$$\mathbf{Y_1} = \mathbf{Xa} \tag{3.3}$$

$\mathbf{Y}_1$ is the output of the first block and **a** are the coefficients. Here **X** is the matrix of input samples provided to the model and is given by

$$\mathbf{X} = \begin{pmatrix} \mathbf{x}_{j,0}(1) & \mathbf{x}_{j,1}(1) & \cdots & \mathbf{x}_{j,M}(1) \\ \mathbf{x}_{j,0}(2) & \mathbf{x}_{j,1}(2) & \cdots & \mathbf{x}_{j,M}(2) \\ & \vdots & & \\ \mathbf{x}_{j,0}(N) & \mathbf{x}_{j,1}(N) & \cdots & \mathbf{x}_{j,M}(N) \end{pmatrix} \tag{3.4}$$

where

$$\mathbf{x}_{j,m}(P) = [x(P-m) \cdots\cdots x(P-m) \,|\, x(P-m)|^j], \quad P \in \mathbb{N} \tag{3.5}$$

While eq. 3.2, in matrix notation, can be written as

$$\mathbf{Y_2} = \mathbf{Vb} \tag{3.6}$$

$\mathbf{Y}_2$ is the output of the second block and **b** are the coefficients.

$$\mathbf{V} = \begin{bmatrix} \mathbf{v_1} & \mathbf{v}^*_1 & \mathbf{1} \end{bmatrix} \tag{3.7}$$

This formation of matrix **V** i.e. appending the conjugate of the input samples with the actual data forms the basis of *I*/*Q* imbalance compensation

$$\mathbf{v_1} = \begin{pmatrix} \mathbf{y}_1^{k,0}(1) & \mathbf{y}_1^{k,1}(1) & \cdots & \mathbf{y}_1^{k,M'}(1) \\ \mathbf{y}_1^{k,0}(2) & \mathbf{y}_1^{k,1}(2) & \cdots & \mathbf{y}_{1'}^{k,M'}(2) \\ & \vdots & & \\ \mathbf{y}_1^{k,0}(N) & \mathbf{y}_1^{k,1}(N) & \cdots & \mathbf{y}_1^{k,M'}(N) \end{pmatrix} \tag{3.8}$$

where

$$\mathbf{y}_1^{k,m'}(N) = [y_1(N-m') \cdots\cdots y_1(N-m') \,|\, y_1(N-m')|^k] \tag{3.9}$$

$\mathbf{Y_2}$ is the final output of the model and is provided to the power amplifier to obtain the linearized and compensated signal.

3.2.1 Coefficients/Parameter extraction

Coefficient extraction in the inverse modeling algorithm is a very important step in trying to compensate for different aforementioned imperfections. The complex valued coefficients of the model can be calculated using the linear least square approach. The coefficients of the first block are given by

$$\hat{\mathbf{a}} = (\mathbf{X}^H \mathbf{X})^{-1} \mathbf{X}^H \mathbf{Y} \tag{3.10}$$

while for the second block the coefficients are given by

$$\hat{\mathbf{b}} = (\mathbf{V}^H \mathbf{V})^{-1} \mathbf{V}^H \mathbf{Y} \tag{3.11}$$

Moore-Penrose pseudo inverse is used to obtain the complex valued parameters provided in eqs. 3.10 and 3.11. Singular value decomposition method is used for the inversion of matrix and is required to calculate the Moore Penrose Pseudo inverse. Calculating the inverse of the matrix is a complexity problem as will be detailed in section 3.4. Also, it is important to note that one needs to have information only about the PA input and output characteristics for extracting the coefficients which consequently generate $\mathbf{Y_1}$ and $\mathbf{Y_2}$ i.e. once the input and the output of the power amplifier are calculated both set of coefficients can be obtained from these without require

any further measurements. The number of complex valued coefficients for the proposed model is $\{(N+1)\times(M+1)\}+\{(K+1)\times(M'+1)\}\times 2+1$. A mentioned earlier, inverting the matrix is a complexity problem and if the dimensions of the matrix are large, the complexity of the system increases enormously.

3.3 Model Performance and Simulation results

As mentioned in chapter one and two, NMSE and ACEPR are the main figures of merit considered in this work for performance evaluation. Fig. 3.4 shows the performance of the distributed model for WCDMA 101 signal having a gain and phase imbalance along with a dc offset. It can be seen that if only the first block is employed (red curve) i.e. if we only compensate for the power amplifier nonlinear effects, the architecture is incapable of proper invers modeling as indicated by the reasonably high error. However, as we introduce the second block which helps to mitigate the effect of *I*/*Q* imbalance, the performance of the system improves considerably. This performance improves even more as the memory depth and the nonlinearity order of the second block is further increased, as it now compensates for the residual nonlinearity of the first block and adding more memory helps to mitigate the effect of the frequency dependent mismatch. Figs. 3.5 to 3.7 show the power spectral density of the error for WCDMA 101, WCDMA 111 signal WCDMA 1111 signals respectively. WCDMA 101 signal has a Peak to Average Power Ratio (PAPR) of 10.61 dB, WCDMA 111 signal has a PAPR of 10.58 dB and WCDMA 1111 signal have a PAPR of 11.27 dB. A gain imbalance of 1 dB and a phase imbalance of 3 degrees is introduced in the signal to emulate the effect of *I*/*Q* imbalance. Also a dc offset of 1% in the in phase component and 1.5% in the quadrature phase component is introduced to emulate the effect of LO leakage. It can be seen in the figures that if we do not

compensate the effect of *I*/*Q* imbalance i.e. if the second block is not considered (red curves), the error increases significantly. However, by employing the proposed architecture (blue curve), the error in the system is reduced considerably. As mentioned earlier, the proposed model is compared with the Parallel Hammerstein based Model. For a fair comparison, both the models evaluated in tables 3.1 and 3.2 were trained with the same number of data samples i.e. 10,000 samples and tested for 25,000 data samples. One effect of the mismatch is that it creates mirror frequency interference [17, 18].

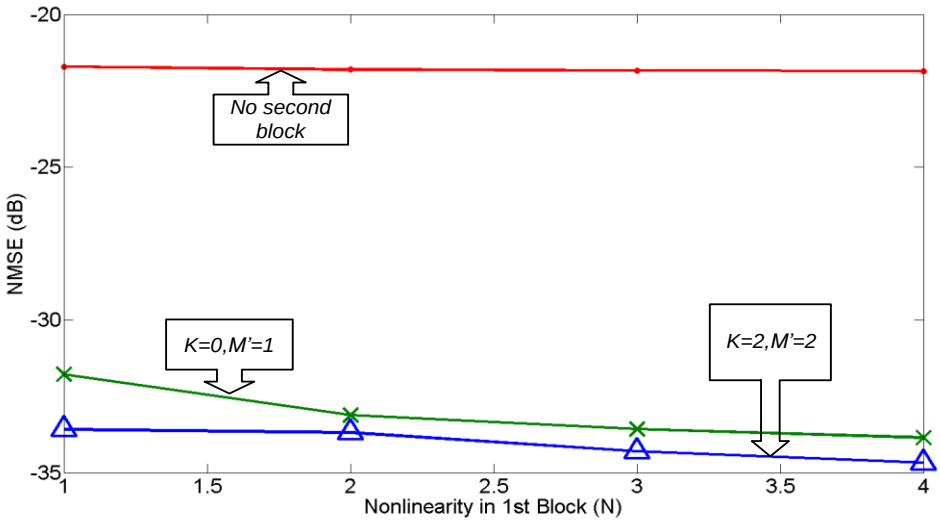

Figure 3.4: Effect of Block 2 on the NMSE of the system for the proposed model for WCDMA 101 signal with *I*/*Q* imbalance and dc offset.

In symmetric signals (i.e. signals that are symmetric around the centre frequency) these effects might not be visible in the spectrum as the image lies directly on the original signal. Hence, as shown in figure 3.1, an asymmetric WCDMA 1101 signal with a centre frequency of 1.96 GHz was generated in order to see the effect of the in band distortion caused by formation of image (encircled in fig. 3.8) at the output of the power amplifier (green curve) due to *I*/*Q* imbalance.

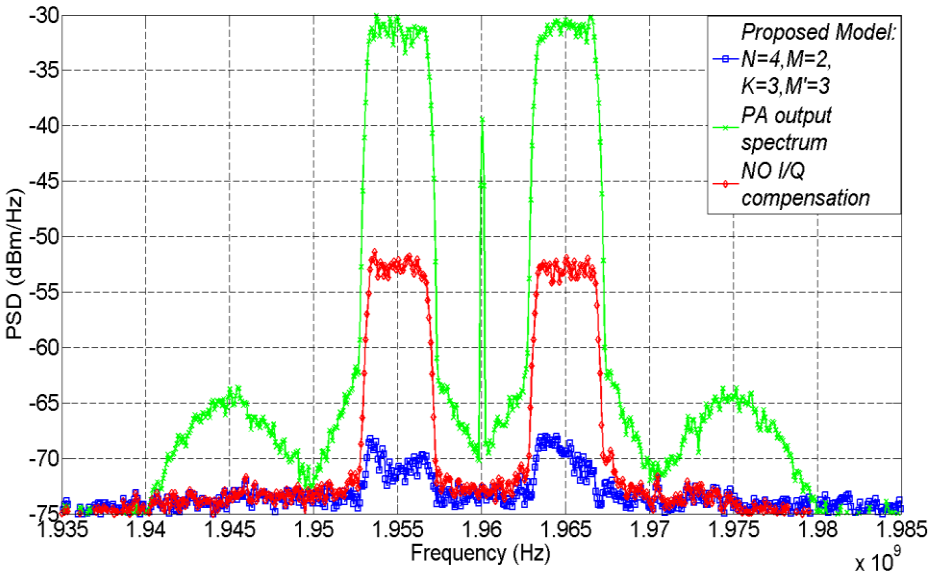

Figure 3.5: Power spectral density of PA output and modeling error for WCDMA 101 signal.

It can be seen that if we do not compensate for the *I*/*Q* imbalance, the model is incapable of removing the image (shown in red curve) caused by the imbalance. However, the proposed model is able to linearize the signal quite remarkably indicating that the model is capable of modeling the inverse PA characteristics and compensate for *I*/*Q* imbalance quite significantly.

3.4 Complexity

At this stage, a question of complexity might arise in the mind of the readers. As mentioned in chapter one that the importance of complexity in digital predistortion design cannot be ignore in modern systems. The proposed model particularly deals with reducing the complexity of the system while maintaining reasonable performance. The figures of merits used in this work for complexity evaluation and numerical stability are dispersion coefficients, condition number, and number of coefficients and floating point operations (FLOPs) required implementing the model.

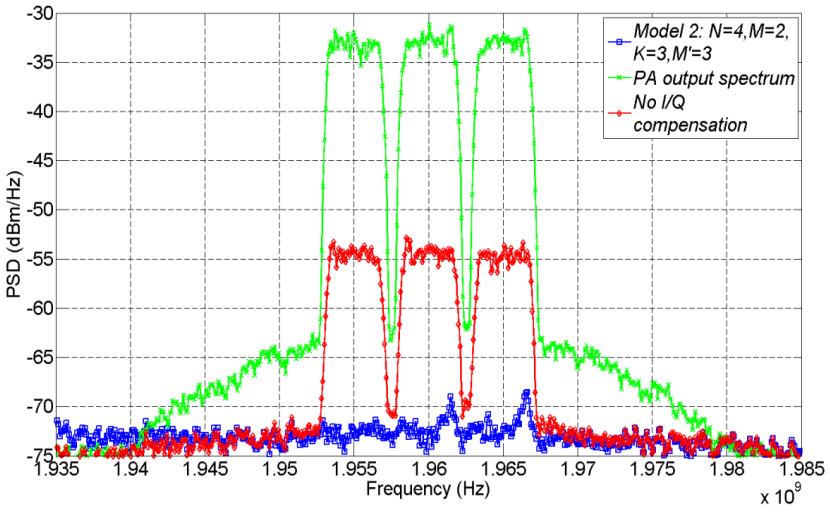

Figure 3.6: Power spectral density of PA output and modeling error for WCDMA 111 signal.

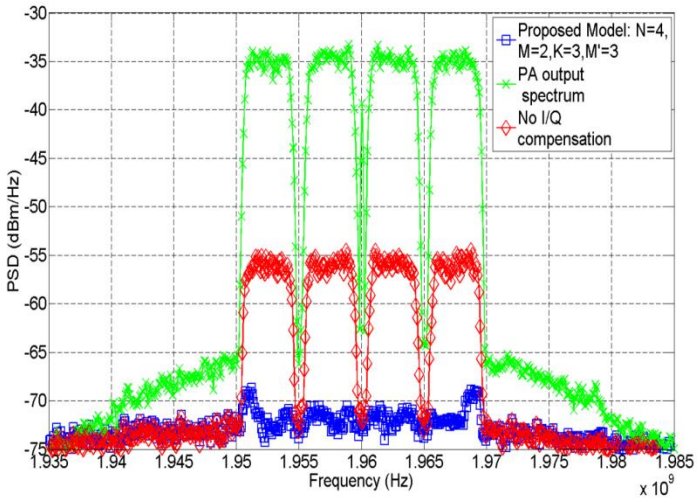

Figure 3.7: Power spectral density of PA output and modeling error for WCDMA 1111 signal.

These have been defined and explained in chapter one of the thesis. FLOPs have been calculated at various stages in the design.

3.4.1 Condition Number and Dispersion Coefficients

Penrose Moore pseudo inverse is used to calculate the inverse of the matrix (in our case **X** and **V**) in order to find the complex valued coefficients of the model in eqs. 3.10 and 3.11. This pseudo inverse is however, sensitive to the changes in the matrix conditioning [33], [36]. Dispersion coefficient, on the other hand, determines the spread of coefficients over the domain number of required bits to fill the domain of coefficients [33]. Tables 3.1 and 3.2 show the complexity of the model and compare it to the previously proposed Parallel Hammerstein (PH) model. In order to fully appreciate the advantage of the proposed models over the existing techniques, one has to consider the above mentioned metrics. It can be seen in table 3.1 that by distributing the nonlinearity and memory depth, the matrix conditioning and dispersion coefficients reduced significantly. For example, for WCDMA 1111 signal the condition number is improved by 33 dB for the proposed model as compared to the PH model. Similarly, the dispersion coefficient is reduced as low as 42 dB which is a quite significant reduction in complexity.

3.4.2 FLOPs for calculating matrix inverse

Another important figure of merit for complexity evaluations is the number of floating point operations (FLOPs) required to compute the model. The FLOPs calculations are done at various stages of computation. For, matrix inversion, Moore-Penrose pseudo inverse is calculated using singular value decomposition (SVD), which according to [49] is a two phase/step process. The first step is reducing the matrix e.g. $A_{u,v}$ into bi-diagonal matrices, the running time for which is $O(uv^2)$ FLOPs (where the O notation is the measure of the running time of an algorithm). In the

second step the bi-diagonal matrix is then diagonal-ized, the computation time for which (for machine epsilon $\varepsilon_{\text{machine}}$) is $O(vlog(|log(\varepsilon_{machine})|))$ FLOPs, which is slower than that of the first step. Hence the running time of SVD algorithm is $O(uv^2)$ FLOPs. In our case, matrices **X** and **V** require inversion during coefficient extraction. During matrix construction, the number of rows depends on the data points chosen and the number of columns depends upon the nonlinearity order and memory depth of the respective block. As indicated above, the number of FLOPs increase as a square of the number of columns, hence by reducing the number of columns (as attained by the proposed model and shown in Table 3.2) the running time is reduced significantly.

3.4.3 FLOPs for matrix-coefficients multiplication

Eqs. 3.3 and 3.6 show that after the coefficients are generated, the original matrices are multiplied by the coefficient vector. For rectangular matrices multiplication [48] e.g. $\mathbf{A}_{m\times n}\times B_{n\times p}$, the running time is bounded by $O(mnp)$. Again we see that by reducing the number of coefficients the running time of the system can be reduced.

3.4.4 FLOPs for calculating the outputs of the blocks ($y_1(n)$ and $y_2(n)$)

The method employed in [47] is used to calculate the number of FLOPs (floating point operations) required to compute the respective polynomial models of both the blocks. For e.g. for the memory polynomial series for one memory index 'm' and nonlinearity order 2 can be written as $a_{0,m}x(n\text{-}m)+a_{1,m}x(n\text{-}m)|x(n)|+a_{2,m}x(n\text{-}m)|x(n\text{-}m)|^2$. Here, since both are complex integers, 6 FLOPs are required to compute $a_{0,m}x(n\text{-}m)$, 2 FLOPs for $x(n\text{-}m)|x(n)|$ i.e. multiplication of a complex integer with a real integer, and then 6 FLOPs for multiplying the product with a1,m. Similarly, $|x(n\text{-}m)|^2$ requires 3 FLOPs, multiplying it with $x(n\text{-}m)$ requires 2 FLOPs and 6 FLOPs for multiplication with $a_{2,m}$. Finally since all these terms are added together so addition of the

terms require another 4 FLOPs. Hence the total number of FLOPs are 29 × (M + 1), where M is the total memory depth. From the above calculations, we can see that by employing these distributed systems we are able to reduce the number of FLOPs at every step of computation. These results are summarized in Table 3.2.

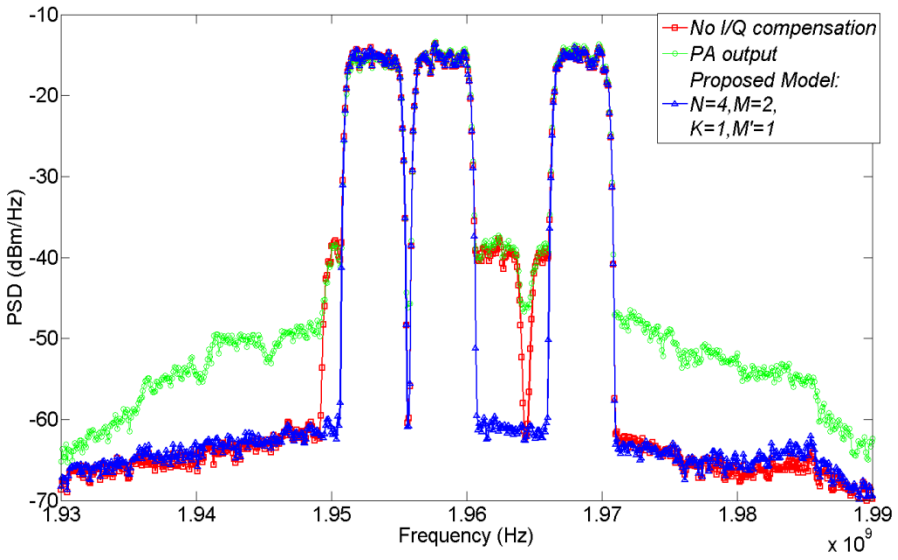

Figure 3.8: Power spectral density of PA output and modeled output of proposed model for WCDMA 1101 signal.

Table 3.1: Complexity Analysis and stability of the proposed model and its comparison to the PH model [32]

Input Signal	Proposed Model *(N=4,M=2,K=2,M'=2)*					PH Model [32] *(memory=4,nonlinearity=5/3)*		
	Dispersion coefficient (dB)		Condition Number (dB)		NMSE (dB)	Dispersion coefficient (dB)	Condition number (dB)	NMSE (dB)
	a	b	X	V				
WCDMA 101	48.3	31.1	68.5	48.8	-34.67	67.32	81	-35.1
WCDMA 111	49.2	32.3	69.7	50.0	-34.38	67.63	82.6	-34.9
WCDMA 1111	51.1	25.3	68.3	47.6	-34.75	67.42	81	-35.2

Table 3.2: Complexity Analysis of the proposed model and its comparison to the PH model [32] in terms of no. of coefficients and FLOPs

Metric	Proposed Model	PH Model	% reduction
			Proposed Model
Coefficients	34	41	17
FLOPs	333	400	16.7
Running time for SVD in terms of FLOPs for N data samples			
Proposed Model			**PH Model**
X	**V**		**Matrix to be inverted**
$O(225\times N)$	$O(361\times N)$		$O(1681\times N)$
Running time for matrix-coefficients multiplication for N data samples			
Proposed Model			**PH Model**
Xa (eq. 3.3)	**Vb (eq. 3.6)**		**Matrix×vector**
$O(15\times N)$	$O(19\times N)$		$O(41\times N)$

3.5 Measurement Results

The digital predistortion is carried out using the indirect learning architecture (ILA) in which first iteration requires inverse modeling of the system. The before mentioned class AB power amplifier with a maximum power of 3 dBm is fed by a WCDMA 1101 signal with a centre frequency of 1.96 GHz and a peak-to- average power ratio (PAPR) of 12 dB. A gain imbalance of 1 dB and a phase imbalance of 3 degrees are created in the input signal along with a dc offset of 1 % in the in-phase and 1.5% in the quadrature-phase component, which is then fed to the models which generate a predistorter signal. The predistorted signal is then fed to a class AB PA and the linearized signal is captured using a vector signal analyzer (Agilent E4440A). Fig. 3.9 shows the measured power spectral density of the linearized signal using the proposed model and the PH model. The model shows reasonable ACPR with reduced complexity which essentially meets the desired purpose of the proposed method i.e. keeping similar performance while

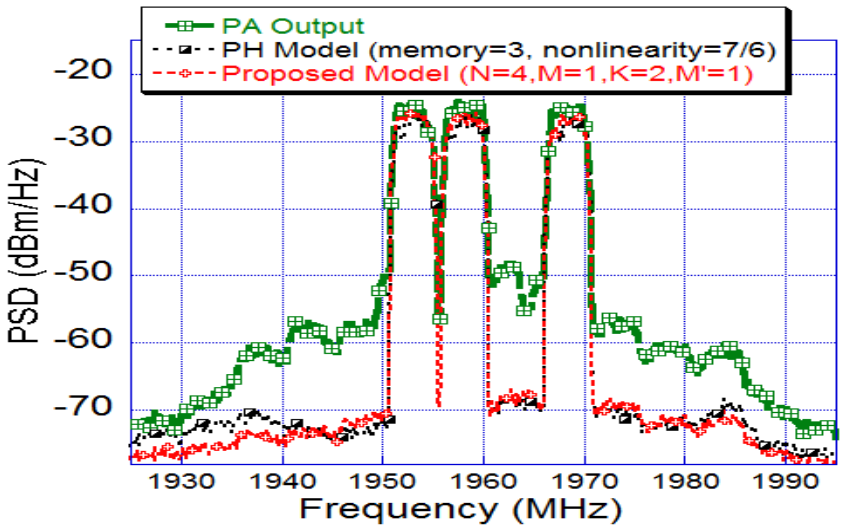

Figure 3.9: Power spectral density of PA output and proposed model (23 coefficients) and comparison to the PH Model [32] (53 coefficients) for WCDMA 1101 signal.

reducing the coefficients, condition number and dispersion coefficients significantly as compared to the PH model (53 coefficients).

3.6 Conclusion

In this chapter, we explored a novel memory polynomial based distributed model for the mitigation of PA nonlinearity and *I*/*Q* mismatch. Various figures of merit and experimental results show that the model is able to reduce the complexity significantly, while maintaining reasonable performance. Number of coefficients and associated complexity is much lower as compared to PH model, without losing any in-band-performance performance and out-of-band performance.

Chapter four: Discussion and Future Work

4.1 Discussion regarding proposed work

Throughout this thesis we investigated the behavioral modeling of the power amplifiers as they are one of the basic components in any communication system as their nonlinear characteristics give rise to intermodulation distortions and degrade the transmitter's performance. An extensive literature has been reviewed to understand the problems in direct conversion transmitters and investigate various methods that mitigate these. As it has been mentioned in chapter one of the thesis that several methods aim to alleviate the degrading effects of the power amplifier. However, it is not the only problem that a transmitter faces. In addition to this the problem of *I*/*Q* imbalance due to the mixer cannot be neglected in real systems and it has been shown that models that only consider the effect of power amplifier are incapable of proper modeling in the presence of *I*/*Q* imbalance. Hence this thesis aimed to consider the effects of *I*/*Q* imbalance along with PA nonlinearity. In this thesis we presented two digital predistortion models to mitigate various imperfections in direct conversion transmitters. Both models were evaluated on the basis of performance and complexity and were compared to the Parallel Hammerstein based model. Rational Function based model has a better performance than the PH model, however this came at the expense of higher complexity. However, it was shown that as we reduced the nonlinearity and the memory depth of the model the complexity reduced. Distributed two block model on the other hand had a similar performance to the PH model however it has a very low complexity.

In our continuing and future work, we wish to explore other models and investigate further into other limitations in transmitters. One work can be to study the difference between time and frequency domain methods. Also, in the modern age energy efficiency has also become an

enormous concern. Hence one can also investigate and work on models that are more energy efficient. The literature reviews and explanations of these works are provided in the next sections.

4.2 Frequency Domain Predistortion - Literature Review

All the methods proposed in this work are time domain methods employing indirect learning architecture for the alleviation of various direct conversion transmitter imperfections. However there are various methods found in literature which employ a frequency domain analysis for the same purpose. The authors in [19, 45, and 46] claim that by using a frequency domain measure of the output spectrum the gain/delay compensation errors can be avoided. Also the ADC distortion in the feedback path can be avoided. The time delay effect has been elaborated in [19] according to which it is caused by the transmission and receiving filters. In our future work, we wish to explore various advantage and drawbacks of various frequency domain methods and compare them with time domain methods. Figs. 4.1 and 4.2 show the block diagram of time domain and frequency domain predistortion models.

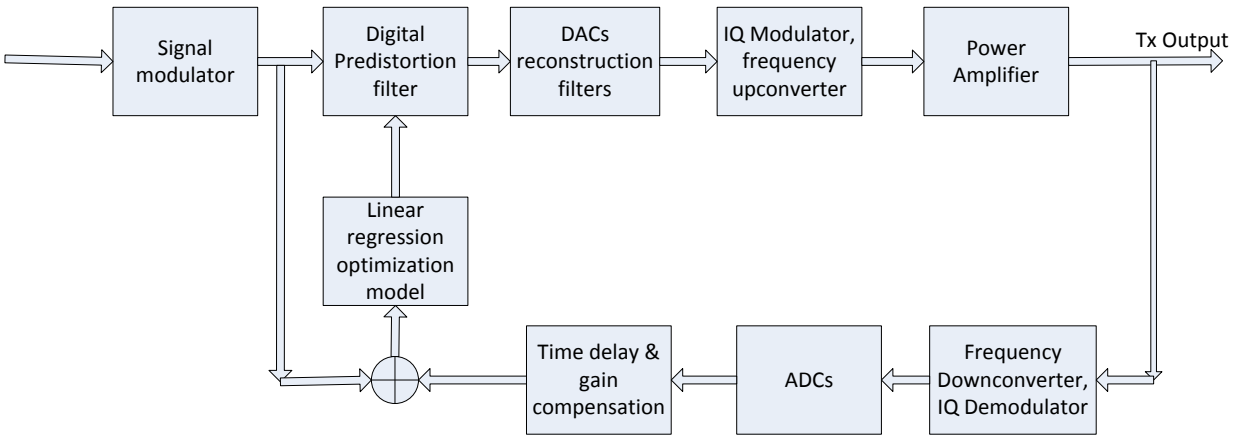

Figure 4.1: Time domain based digital predistortion (@ 2008 IEEE [19])

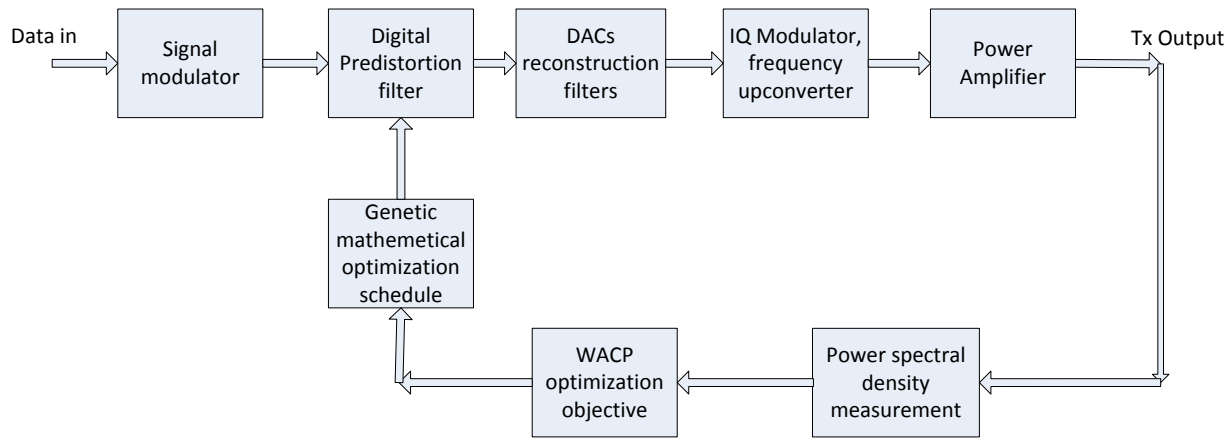

Figure 4.2: Frequency domain based digital predistortion (@ 2013 IEEE [46])

The model presented in [19] employs various predistortion algorithms for the linearization of power amplifiers namely Zero-Forcing algorithm, PA-Input-LS algorithm, Adaptive PA-Input-LS algorithm, Adaptive Finite-Difference algorithm and Adaptive Secant Algorithm. The method proposed in [19] is as follows: As mentioned in eq. 1.22 that an inverse static PA model with only odd orders can be given by

$$PA^{-1}: x(n) = d_1 y(n) + d_3 y(n) | y(n) |^2 + ... \quad (4.1)$$

Where $x(n)$ is the input to the signal and $y(n)$ is the output. In any inverse modeling algorithm, we wish to estimate $x(n)$ which gives the least error.

$$\hat{x}(n) = d_1 y(n) + d_3 y(n) | y(n) |^2 + ... \mathrm{d}_{2\mathrm{m}-1} \mathrm{y}(n) | \mathrm{y}(n) |^{2\mathrm{m}-2} \quad (4.2)$$

Where $\mathbf{d} = [d_1 \ d_3 \ \ldots\ldots \ d_{2m-1}]$ are the coefficients of the model and m is the nonlinearity order. Taking the N point DFT, the frequency domain expression of the above equation is given by

$$\hat{X}(\mathrm{k}) = d_1\,\mathrm{Y}_1(k) + d_3 Y_3(k) + \ldots\ldots\ldots\mathrm{d}_{2\mathrm{m}-1}\,Y_{2m-1}(k) \tag{4.3}$$

$$\hat{X}[\mathrm{k}] = FFT\{\hat{\mathrm{x}}(\mathrm{n})\} \tag{4.4}$$

Similarly

$$Y_j(k) = \mathrm{FFT}\{\mathrm{y(n)}\,|\,\mathrm{y(n)}\,|^{j-1}\} \tag{4.5}$$

In matrix notation, eq. 4.2 can be written as

$$\mathbf{X} = \mathbf{Yd} \tag{4.6}$$

where

$$Y = \begin{bmatrix} Y_1(k_1) & Y_3(k_1) & .... & Y_{2m-1}(k_1) \\ Y_1(k_2) & Y_3(k_2) & .... & Y_{2m-1}(k_2) \\ \vdots & \vdots & & \vdots \\ Y_1(k_m) & Y_3(k_m) & .... & Y_{2m-1}(k_m) \end{bmatrix} \tag{4.7}$$

From eq. 4.6, we can extract the coefficients of the matrix, which can be given by

$$\mathbf{d} = \mathbf{Y}^{-1}\mathbf{X} \tag{4.8}$$

Here the matrix **Y** has to be a square matrix, in order to compute the inverse. Hence this method tries to compute the inverse PA characteristics in frequency domain to avoid the gain/delay mismatch phenomena which is present in its time domain counterpart. However, the method is quite similar to the one generally used in time domain predistortion methods. This was the zero forcing Algorithm. In addition to this the authors have also applied other algorithms namely, PA-Input-LS Algorithm, Adaptive PA-Input-LS algorithm, Adaptive Finite-Difference algorithm and Adaptive Secant Algorithm. However, these methods focus only on the nonlinear behaviour of the power amplifier. Whereas in real systems,, the presence of *I*/*Q* imbalance due to the mixer

affects the performance of these methods. Hence, these effects should be considered as well. Eq. 1.20 provides the *I*/*Q* imbalance model in frequency domain. Since this work focuses on OFDM signals, so the *I*/*Q* imbalance model for OFDM signals is as follows [45]

$$Y(k) = \mathrm{G}_1(k)\,\mathrm{X}(k) + \mathrm{G}_2(k)\,\mathrm{X}^*(-k) \tag{4.9}$$

Where X(*k*) is the baseband signal to be transmitted and Y(*k*) denotes the transmitted signal containing the effect the of imbalance. Here *k* denotes the OFDM subcarrier index. *Hence investigating the effects of I/Q imbalance and how the existing frequency domain based methods get affected by it is a serious problem and we wish to examine this in our future work.* Another digital predistortion method introduced in [45, 46] for high crest factor applications such as DAB, DVB-T and WCDMA transmitters also employs a frequency domain measure. According to the authors, this method is different from the traditional time domain approaches because of two main factors: Firstly, there is no need for gain/delay compensation as is required for time domain techniques and secondly it models the predistortion filter parameters as an optimization problem rather than a linear regression problem. In this method, the authors use a frequency domain measure to linearize the system, specifically Weighted Adjacent Channel Power (WACP) and try to find the optimal weights/parameters/coefficients to reduce this function. One important method introduced by the authors is to find the appropriate memory in the system. For this purpose the authors have used a triple pruned Volterra series which considers only the third order coefficient and is given by

$$y(n) = x(n) + h_3(k)x(n)\,|\,x(n-k)\,|^2 \tag{4.10}$$

Here by changing the value of *k* gives the exact memory of the system. After predistortion filter estimation, the authors explain the formation of the optimization vector space ***h*** which is

dominated by the odd order kernels as they affect the performance greater than the even order ones which lie farther away from the band of interest. Finally, a frequency domain measure of the power amplifier output linearity is provided which is named Weighted Adjacent Channel Power (WACP) and is provided by

$$WACP = \sum_{LAC} W(f)P(f) + \sum_{UAC} W(f)P(f) \tag{4.11}$$

The goal is to find the optimal weighting function $W(f)$ that reduces the optimization function. The optimization is done for initial setting (i.e. at the start of the transmitter's operation) and also for on air adaption (i.e. after the transmitter is operational and is affected by various factors such as temperature, component aging etc.).

4.3 Discussion on future work

The methods explained in the previous section proposed various methods which employ frequency domain predistortion. After studying these methods, we wish to explore further into frequency based predistortion and evaluate further its advantages or disadvantages as compared to its time domain counterpart. The methods proposed in [19] employ various adaptive and optimization algorithms to counter the power amplifier nonlinearity issue. However, it can be seen that the issue of I/Q imbalance is not taken into consideration in any of these methods. In addition to this, these methods are complex. In [45, 46], a methods of memory sweep has been introduced to find the appropriate memory in the system by choosing a certain nonlinearity order. However, there are other methods that can be investigated and applied in the frequency domain to find out the appropriate memory and nonlinearity order. One such method is proposed in [44]. Hence, a lot of work can be done in this area to improve the existing predistortion methods and also introduce low complexity model while maintaining the model fidelity.

Another issue that has gained a lot of importance over the years deals with energy efficiency. Various figures of merit have been considered so far, however, over the years, energy efficiency has become an important metric for system designs. In [47], it is shown how the energy is related to the latency and problem size for matrix multiplication. It is shown there that when two n×n matrices are multiplied, the energy of the system increases considerably when he problem size (n) is increased. It is also shown that energy is directly proportional to latency. By definition, latency is defined as the number of clock cycles to complete a single multiplication for a multiplication operation or an entire sum of multiplication computation for multiply and accumulate operation. For e.g. for Altera EP2S15FF484C3 the latency is 7 cycles to compute an entire sum of multiplications for MAC operation, 3 cycles to compute one multiplication. Hence, if the no. of floating point operations increase, the latency of the system increases, this in turn increases the energy of the system.

REFERENCES

[1] D. Theckedath and T. J. Thomas, “The 700 MHz Spectrum Auction,” *Hillnotes*, *Industry, infrastructure and Resource Division*.

[2] M. Rawat, “Artificial Neural Networks for Behavioral Modeling and Digital Predistortion for Software Defined Transmitters”, *Thesis*, Sep. 2012

[3] D. Schreurs, M. O’Droma, A. A. Goacher, and M. Gadringer, *RF Power Amplifier Behavioral Modeling*. Artech House, 2009.

[4] J. C. Pedro and S. A. Maas, "A comparative overview of microwave and wireless power-amplifier behavioral modeling approaches," *IEEE Transactions on Microwave Theory and Techniques*, vol.53, no.4, pp.1150,1163, Apr. 2005.

[5] H. Ochiai, "An Analysis of Band-limited Communication Systems from Amplifier Efficiency and Distortion Perspective," *IEEE Transactions on Communications*, vol.61, no.4, pp.1460-1472, Apr. 2013

[6] S. Mirabbasi and K. Martin, “Classical and modern receiver architectures,” *IEEE Communications Magazine*, vol. 38, no. 11, pp. 132-139, Nov. 2000.

[7] A. A. Abidi, "Direct-conversion radio transceivers for digital communications," *IEEE Journal of Solid-State Circuits*, vol. 30, no.12, pp.1399-1410, Dec 1995

[8] N. Boulejfen, A. Harguem, O. Hammi, F. M. Ghannouchi, A. Gharsallah, "Analytical prediction of spectral regrowth and correlated and uncorrelated distortion in multicarrier wireless transmitters exhibiting memory effects," *IET Microwaves, Antennas & Propagation*, vol.4, no.6, pp. 685-696, Jun. 2010

[9] J. K. Cavers, “The Effect of Quadrature Modulator and Demodulator Errors on Adaptive Digital Predistorters for Amplifier Linearization,” *IEEE transactions on Vehicular Technology*, vol. 46, no. 2, pp. 456–466, May 1997.

[10] Per Landin, “Digital baseband Modeling and Correction of Radio Frequency Power Amplifiers”, *Thesis*, June 2012.

[11] Peter Jantunen, “Modelling of Nonlinear power Amplifiers for Wireless Communications”, *Thesis*, Mar. 2004.

[12] M. Franco, A. Guida, A. Katz, and P. Herczfeld, "Reduction of In-Band Intermodulation Distortion Products in Radio Frequency Power Amplifiers with Digital Predistortion Linearization," *IEEE MTT-S Microwave Symposium Digest*, pp. 918-921, Jun. 2006

[13] I. Takenaka, K. Ishikura, H. Takahashi, K. Hasegawa, K. Asano, N. Iwata, "Improvement of Intermodulation Distortion Asymmetry Characteristics With Wideband Microwave Signals in High Power Amplifiers," *IEEE Transactions on Microwave Theory and Techniques*, vol.56, no.6, pp.1355-1363, June 2008

[14] D. T. Westwick and R. E. Kearney, *Identification of Nonlinear Physiological Systems*, *IEEE*, 2003

[15] A. A. M. Saleh, "Frequency-independent and frequency-dependent nonlinear models of TWT amplifiers," *IEEE Transactions on Communications*, vol. 29, no. 11, pp. 1715–1720, Nov. 1981.

[16] M. Rawat, F. M. Ghannouchi, "A Mutual Distortion and Impairment Compensator for Wideband Direct-Conversion Transmitters Using Neural Networks," *IEEE Transactions on Broadcasting*, vol.58, no.2, pp.168-177, Jun. 2012

[17] J. Tuthill, A. Cantoni, "Efficient compensation for frequency-dependent errors in analog reconstruction filters used in IQ modulators," *IEEE Transactions on Communications*, vol.53, no.3, pp.489-496, March 2005

[18] L. Anttila, M. Valkama, M. Renfors, "Frequency-Selective *I*/*Q* Mismatch Calibration of Wideband Direct-Conversion Transmitters," *IEEE Transactions on Circuits and Systems II: Express Briefs*, vol.55, no.4, pp.359-363, Apr. 2008.

[19] M. C. Chiu, C. H. Zeng, and M. C. Liu, "Predistorter Based on Frequency Domain Estimation for Compensation of Nonlinear Distortion in OFDM Systems," *IEEE Transactions on Vehicular Technology*, vol.57, no.2, pp.882,892, Mar. 2008

[20] M. Isaksson, D. Wisell, and D. Rönnow, "A comparative analysis of behavioral models for RF power amplifiers", *IEEE Transactions on Microwave Theory and Techniques*, vol. 54, no. 1, pp. 348-359, Jan. 2006

[21] F. Taringou, O. Hammi, B. Srinivasan, R. Malhame, and F. M. Ghannouchi, "Behaviour modelling of wideband RF transmitters using Hammerstein–Wiener models", *IET Circuits Devices Syst.*, 2010, 4, (4), pp. 282–290.

[22] T. Liu, S. Boumaiza, F. M. Ghannouchi, 'Deembedding static nonlinearities and accurately identifying and modeling memory effects in wide-band RF transmitters' *IEEE Transactions on Microwave Theory and Techniques*, 2005, 53, (11), pp. 3578–3587

[23] T. Liu, S. Boumaiza, F. M. Ghannouchi 'Augmented Hammerstein predistorter for linearization of broad-band wireless transmitters', *IEEE Transactions on Microwave Theory and Techniques*, 2006, 54, (4), pp. 1340–1349

[24] M. Younes and F. M. Ghannouchi, “An accurate predistorter based on a feed-forward Hammerstein structure”, *IEEE Transactions on Broadcasting*, 2012, 58, (3), pp. 454–461

[25] M. Younes, O. Hammi, A. Kwan, and F. M. Ghannouchi, “An accurate complexity-reduced ‘PLUME’ model for behavioral modeling and digital predistortion of RF power amplifiers”, *IEEE Transactions on Industrial Electronics*, 58, (4), pp. 1397–1405, 2011.

[26] H. Cao, A. S. Tehrani, C. Fager, T. Eriksson, and H. Zirath, "*I*/*Q* Imbalance compensation using a nonlinear modeling approach," *IEEE Transactions on Microwave Theory and Techniques*, vol.57, no.3, pp.513-518, March 2009.

[27] M. Males, J. Tuthill, and A. Cantoni, “The impact of nonlinearity on digital compensation for IQ modulators,” *Workshop in Proc. 6th Baiona Signal Process. Commun*., 2003, pp. 169–174.

[28] L. Ding, Z. Ma, D. R. Morgan, M. Zierdt, and G. Zhou, “Compensation of frequency-dependent gain/phase imbalance in predistortion linearization systems,” *IEEE Transactions on Circuits and Systems*, vol. 55, no. 1, pp. 390–397, Feb. 2008

[29] A. Benveniste, M. Goursat, and G. Ruget, “Robust identification of a nonminimum phase system: Blind adjustment of a linear equalizer in data communications,” *IEEE Transactions on Automation and Control*, vol. 25, no. 3, pp. 385–399, Jun. 1980.

[30] Y. Zou, M. Valkama, and M. Renfors, “Pilot-Based Compensation of Frequency-Selective I/Q Imbalances in Direct-Conversion OFDM Transmitters," *IEEE 68th Vehicular Technology Conference*, pp. 1-5, Sept. 2008

[31] R. K. McPherson, "Frequency-selective I/Q imbalance compensation for OFDM transmitters using online frequency-domain adaptive predistortion," *Military Communications Conference*, pp. 532-537, Nov. 2011

[32] L. Anttila, P. Handel, and M. Valkama, “Joint mitigation of power amplifier and *I*/*Q* modulator impairments in broadband direct-conversion transmitters,” *IEEE Transactions on Microwave Theory and Techniques*, vol. 58, no. 4, pp. 730–738, Apr. 2010.

[33] M. Rawat, F. M. Ghannouchi, and K. Rawat, "Three-Layered Biased Memory Polynomial for Modeling and Predistortion of Transmitters with Memory," *IEEE Transactions Circuits and Systems I: Regular Papers*, vol. 60, no. 3, pp. 768-777, Mar. 2012.

[34] O. Hammi, M. Younes, and F. M. Ghannouchi, “Metrics and methods for benchmarking of RF transmitter behavioral models with application to the development of a hybrid memory polynomial model.” *IEEE Transactions on Broadcasting*, 56(3) (2010), 350–357.

[35] F. M. Ghannouchi and O. Hammi, “Behavioral modeling and predistortion.” *IEEE Microwave Magazine*. vol. 10, no. 7, pp. 52-64, Dec. 2009.

[36] G. H. Golub and C. F. Van Loan, *Matrix computations*, Third Edition, Baltimore, *The John and Hopkins Press Ltd.*, 1996, Chapter 2, pp. 81.

[37] A. S. Tehrani, H. Cao, S. Afsardoost, T. Eriksson, M. Isaksson, and C. Fager, "A Comparative Analysis of the Complexity/Accuracy Tradeoff in Power Amplifier Behavioral Models," *IEEE Transactions on Microwave Theory and Techniques*, vol. 58, no. 6, pp. 1510-1520, Jun. 2010.

[38] O. Hammi and F. M. Ghannouchi, "Twin Nonlinear Two-Box Models for Power Amplifiers and Transmitters Exhibiting Memory Effects With Application to Digital Predistortion," *IEEE Microwave and Wireless Components Letters*, vol. 19, no. 8, pp. 530-532, Aug. 2009.

[39] D. Huang, H. Leung, and X. Huang, "Experimental Evaluation of Predistortion Techniques for High- Power Amplifier," *IEEE Transactions on Instrumentation and Measurements*, vol. 55, no. 6, pp. 2155-2164, Dec. 2006.

[40] H. Paaso and A. Mammela, "Comparison of direct learning and indirect learning predistortion architectures," *IEEE International Symposium on Wireless Communication Systems*, pp. 309-313, Oct. 2008

[41] H. Leung and S. Haykin, "Detection and estimation using an adaptive rational function filter ," *IEEE Transactions on Signal Processing* , vol.42, no.12, pp.3366-3376, Dec. 1994.

[42] S. Mahil, A. B. Sesay, "Rational function based predistorter for traveling wave tube amplifiers," *IEEE Transactions on Broadcasting*, vol. 51, no. 1, pp. 77-83, March 2005.

[43] M. Aziz, M. Rawat, and F. M. Ghannouchi, "Rational Function Based Model for the Joint Mitigation of *I*/*Q* Imbalance and PA Nonlinearity," *IEEE Microwave and Wireless Components Letters*, vol. 23, no. 4, pp. 196-198, April 2013.

[44] M.V. Amiri, S.A. Bassam, M. Helaoui and F.M. Ghannouchi, "New order selection technique using information criteria applied to SISO and MIMO systems predistortion", *International Journal of Microwave and Wireless Technologies*, vol. 5, no. 2, pp. 123-131, April 2013.

[45] B. D. Laki and C. J. Kikkert, "Adaptive Digital Predistortion for Wideband High Crest Factor Applications Based on the WACP Optimization Objective: A Conceptual Overview," *IEEE Transactions on Broadcasting*, vol.58, no.4, pp. 609-618, Dec. 2012

[46] B. D. Laki and C. J. Kikkert, "Adaptive Digital Predistortion for Wideband High Crest Factor Applications Based on the WACP Optimization Objective: An Extended Analysis," *IEEE Transactions on Broadcasting*, vol. 59, no. 1, pp. 136-145, Mar. 2013.

[47] R. Scrofano, S. Choi, and V. K. Prasanna, "Energy efficiency of FPGAs and programmable processors for matrix multiplication," *IEEE International Conference on Field-Programmable Technology*, pp. 422- 425, Dec. 2002.

[48] F. Le Gall, "Faster Algorithms for Rectangular Matrix Multiplication," *IEEE 53rd Annual Symposium on Foundations of Computer Science (FOCS)*, pp. 514-523, Oct. 2012

[49] L. N. Trefethen and D. Bau III, *Numerical linear algebra*, Society for Industrial Applied Mathematics (SIAM) 1997.

[50] M. Younes and F. M. Ghannouchi, "On the Modeling and Linearization of a Concurrent Dual-Band Transmitter Exhibiting Nonlinear Distortion and Hardware Impairments," *IEEE Transactions on Circuits and Systems I: Regular Papers* (online)

[51] M. Rawat, K. Rawat, F. M. Ghannouchi, S. Bhattacharjee, and H. Leung, "Generalized Rational Functions for Reduced-Complexity Behavioral Modeling and Digital Predistortion of Broadband Wireless Transmitters," *IEEE Transactions on Instrumentation and Measurement (online)*.

[52] D. Saffar, N. Boulejfen, F. M. Ghannouchi, M. Helaoui, and A. Gharssalah, "A compound structure and a single-step identification procedure for I/Q and DC offset impairments and nonlinear distortion modeling and compensation in wireless transmitters." *International Journal of RF and Microwave Computer Aided Engineering*, vol. 23, pp. 367–377.